Role of Coherent Vortices on scalar transport and exchange processes within and above the Amazon Forest.

Luca Mortarini

Biosphere-Atmosphere Interaction

The Biosphere-Atmosphere interactions mainly happen inside the **Planetary Boundary Layer** through biogeochemical **fluxes**, where a (**turbulent**) flux is a unifying principle in the transport of mass and energy.

Studying and understanding the Biosphere-Atmosphere interactions is a core activity within the discipline of Earth System Sciences. Many of the most pressing environmental challenges that our society faces together with their remedies, can be traced to the Biosphere-Atmosphere interactions within the Earth System.

Even if the role played by Atmospheric sciences in the history of Natural Philosophy is often underscored, our Atmosphere is crucial for keeping the Earth surface in a Goldilocks position for carbon based life forms (among which… human beings).

Structure of the Planetary Boundary Layer

Idealised PBL

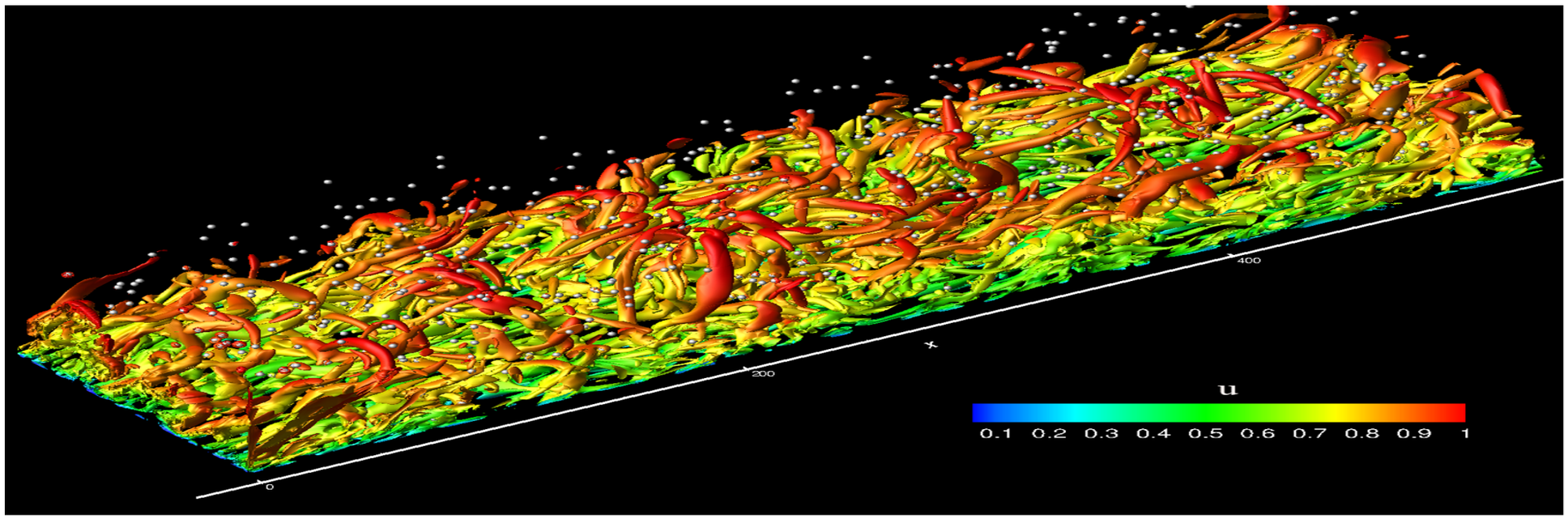

Structure of the Planetary Boundary Layer

Idealised PBL

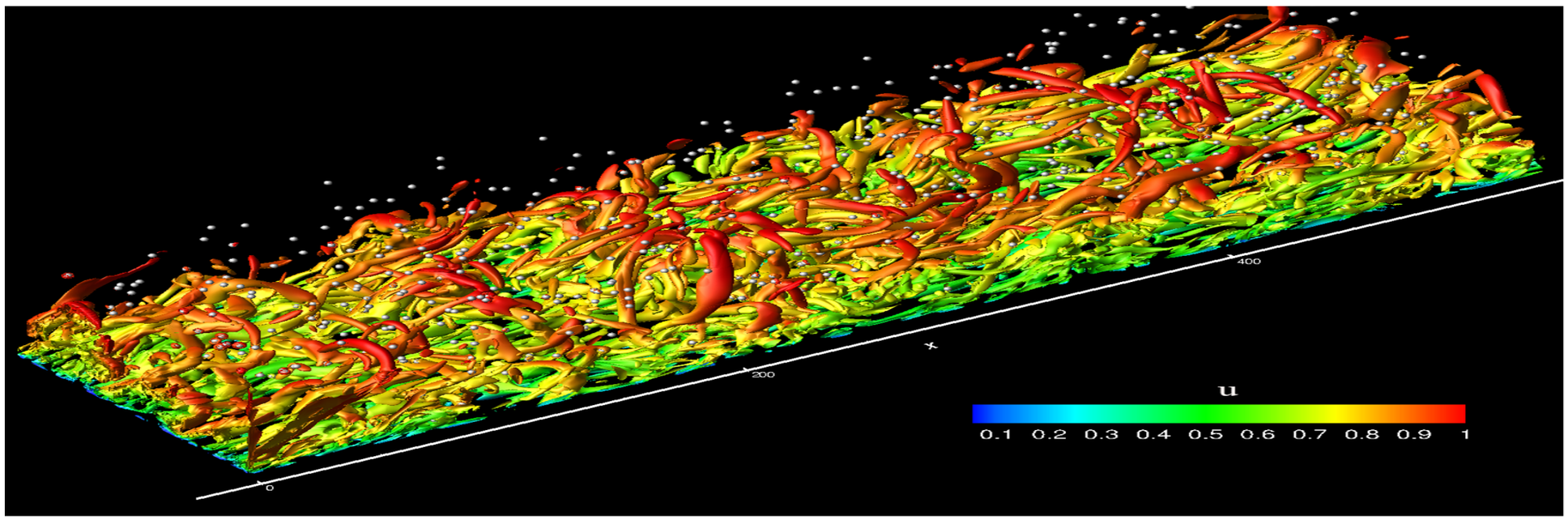

Real PBL

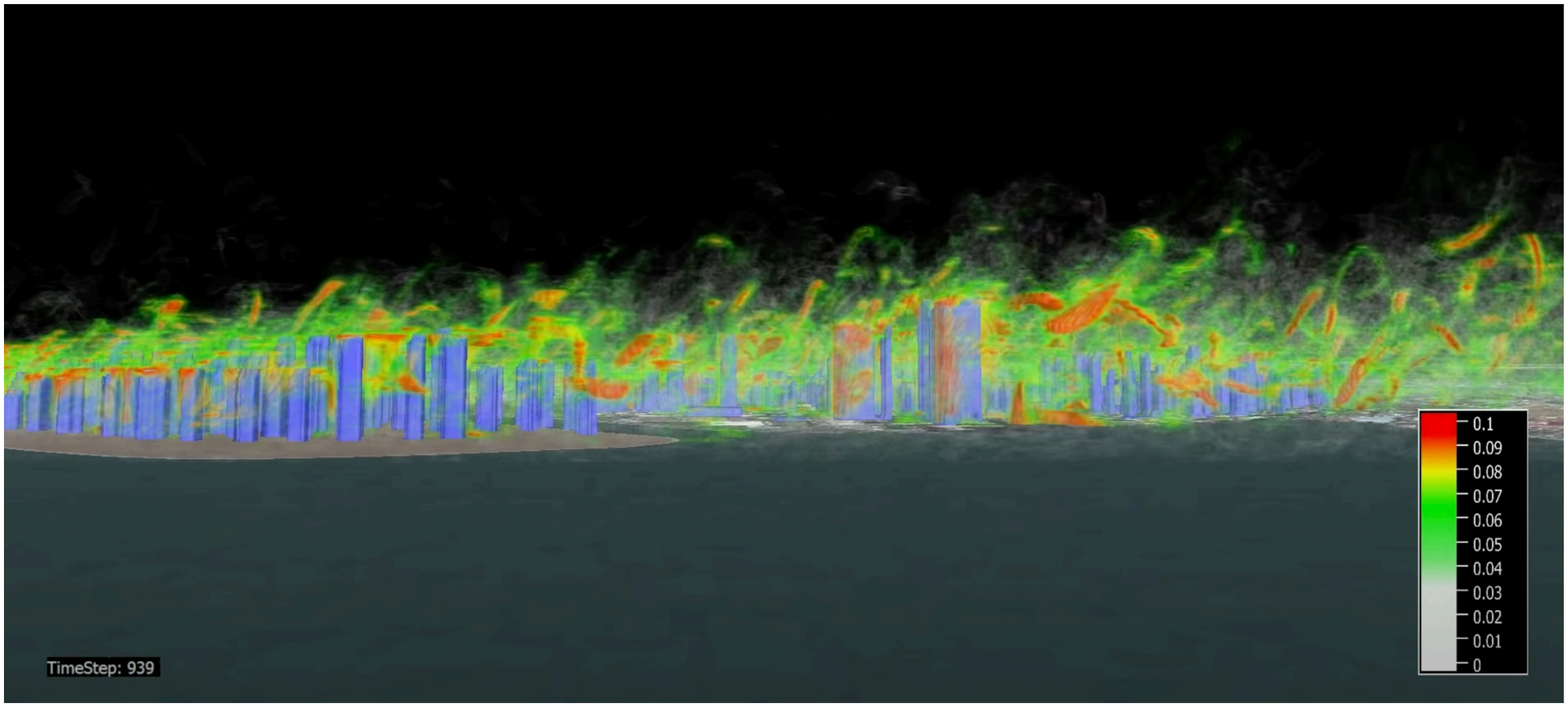

Structure of the Planetary Boundary Layer

Idealised PBL

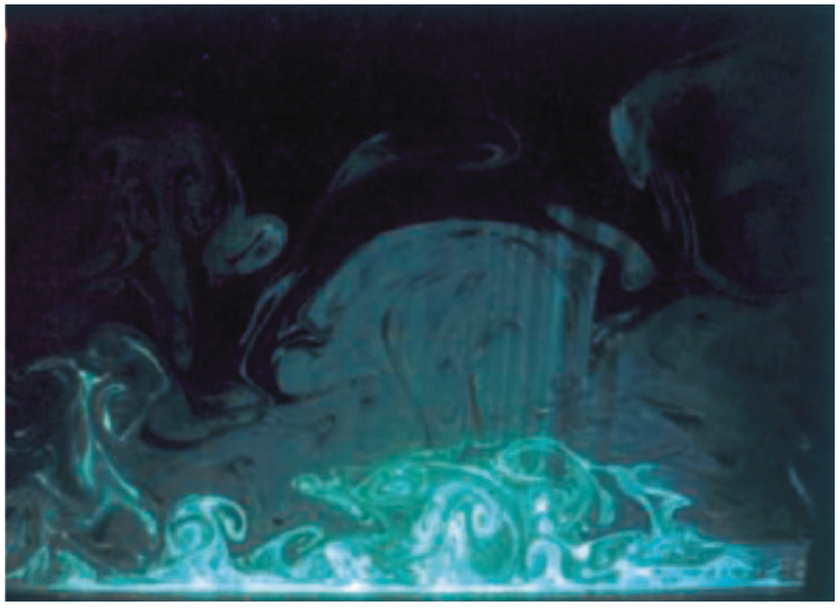

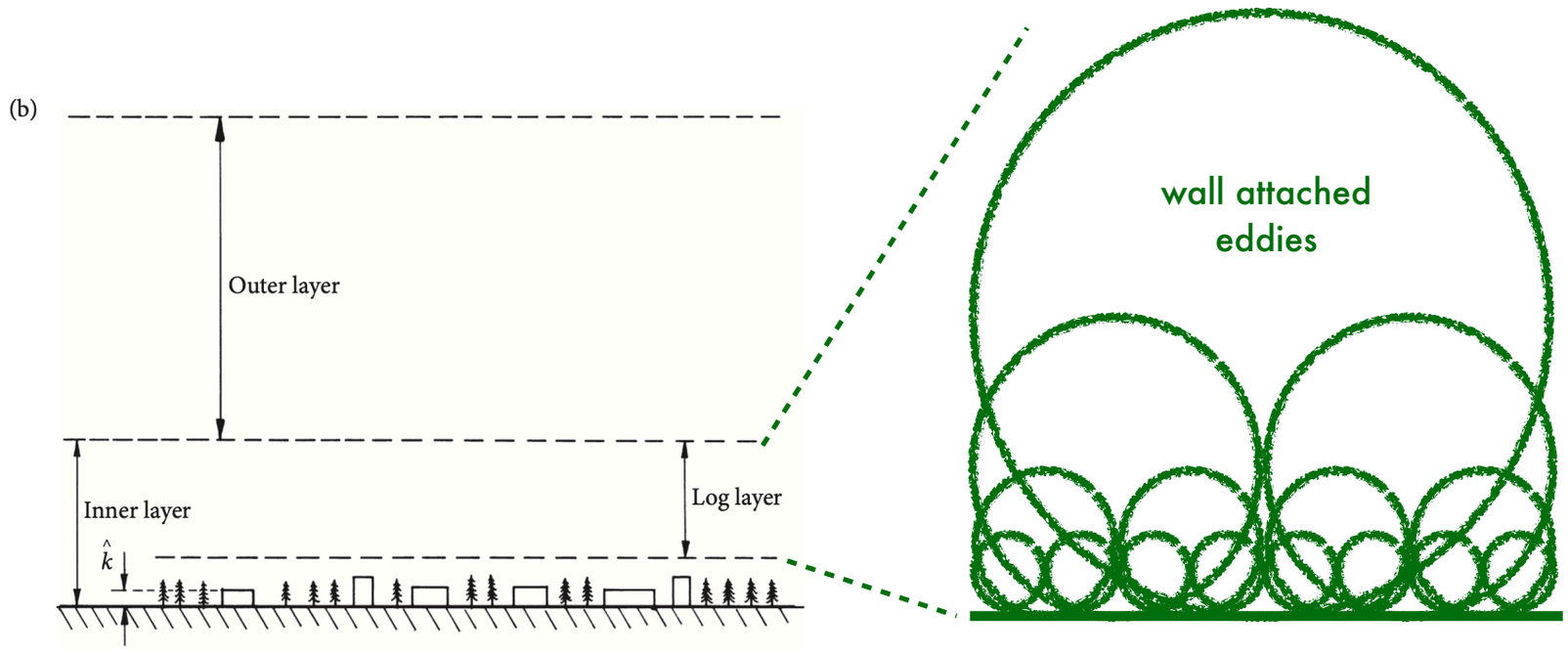

Structure of the Planetary Boundary Layer

Idealised PBL

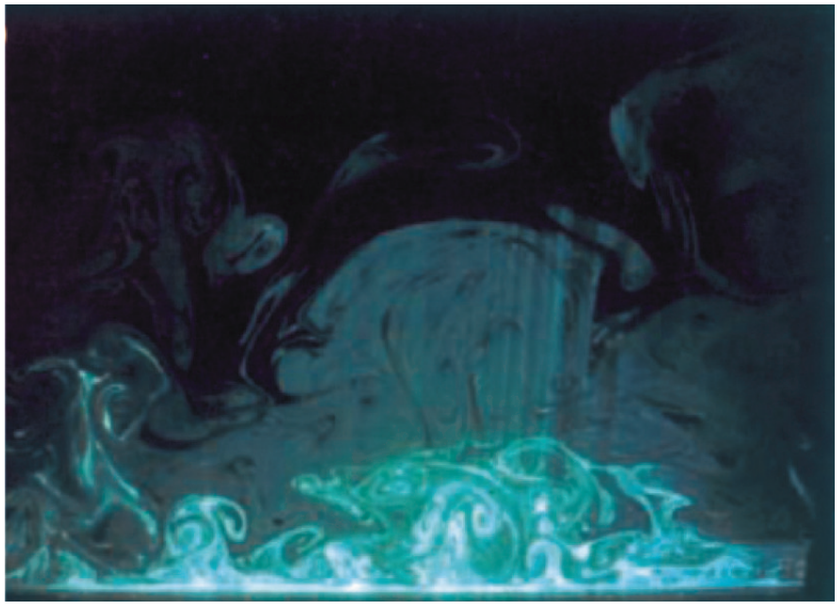

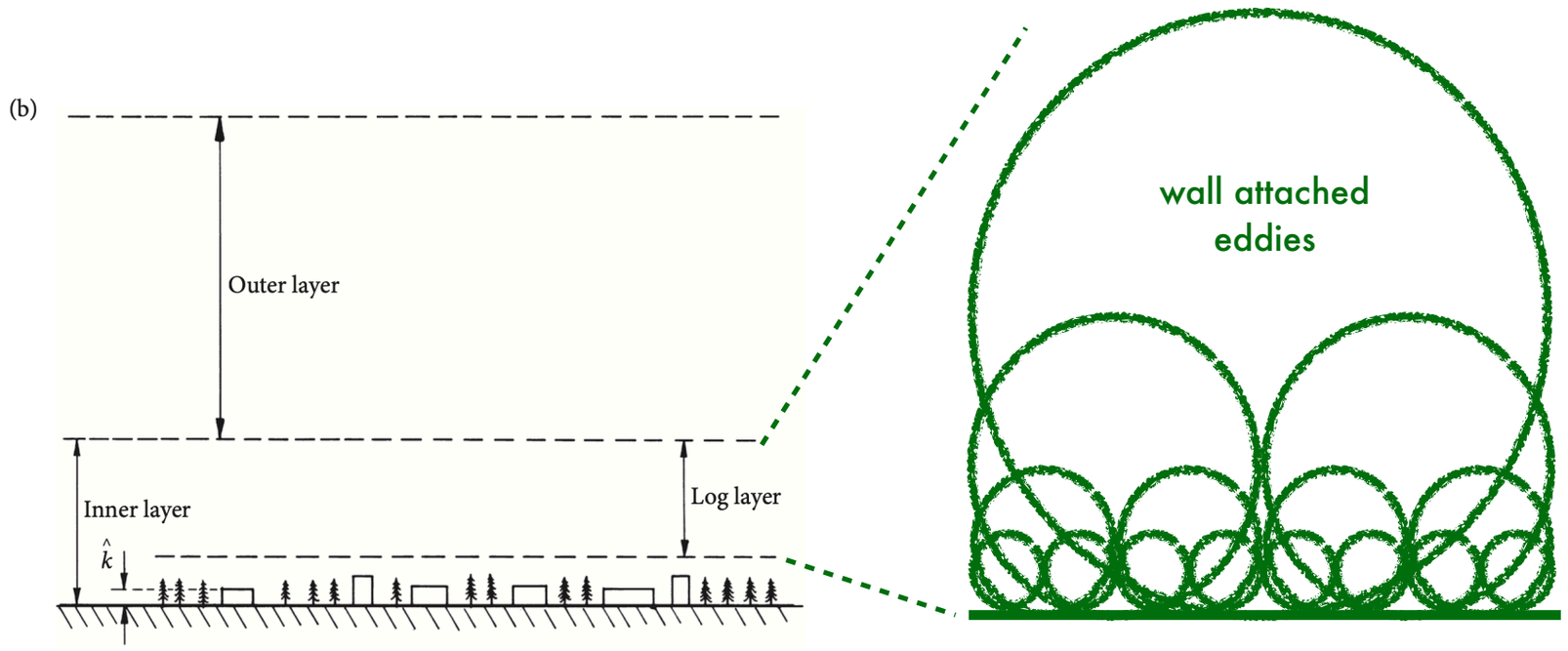

Real PBL

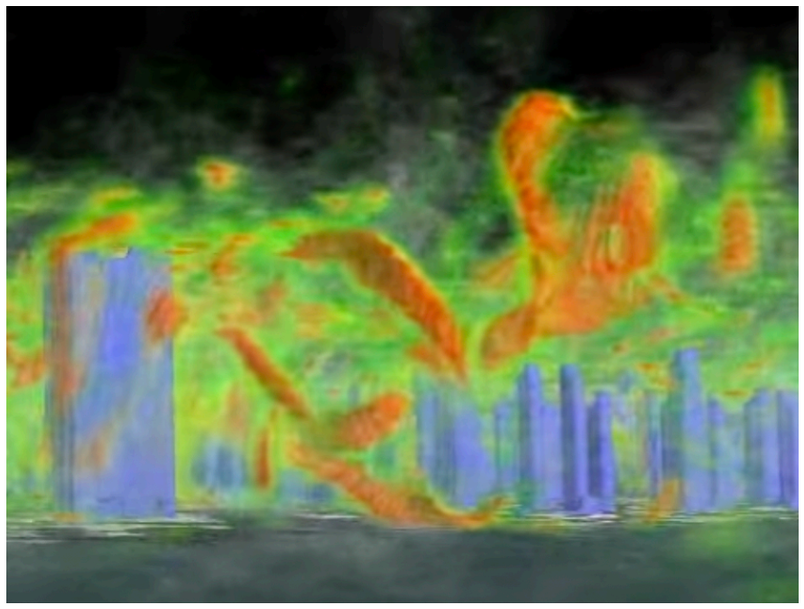

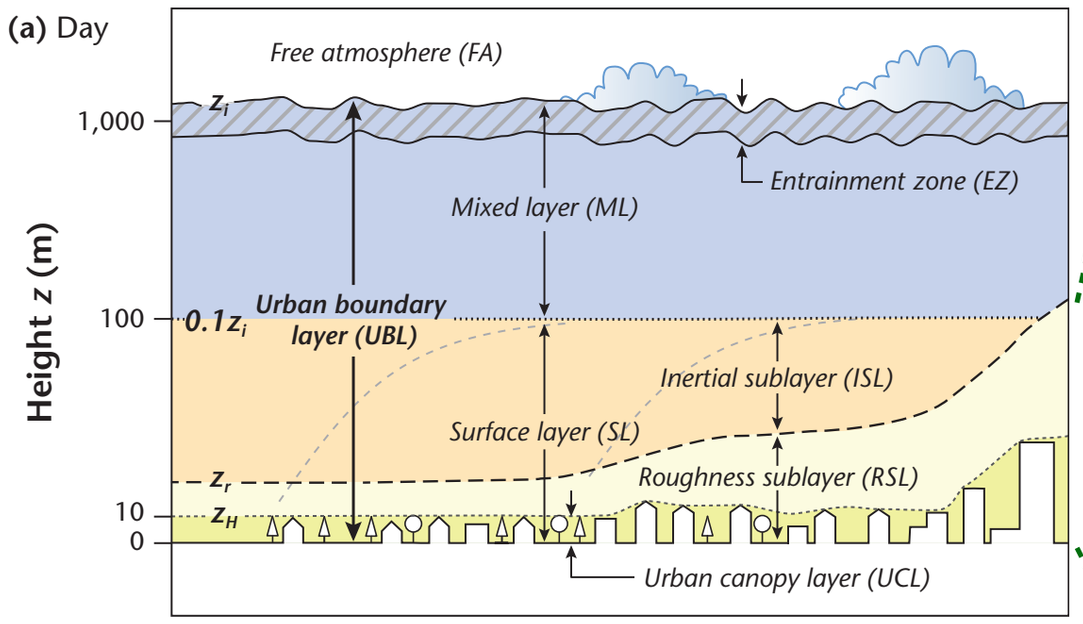

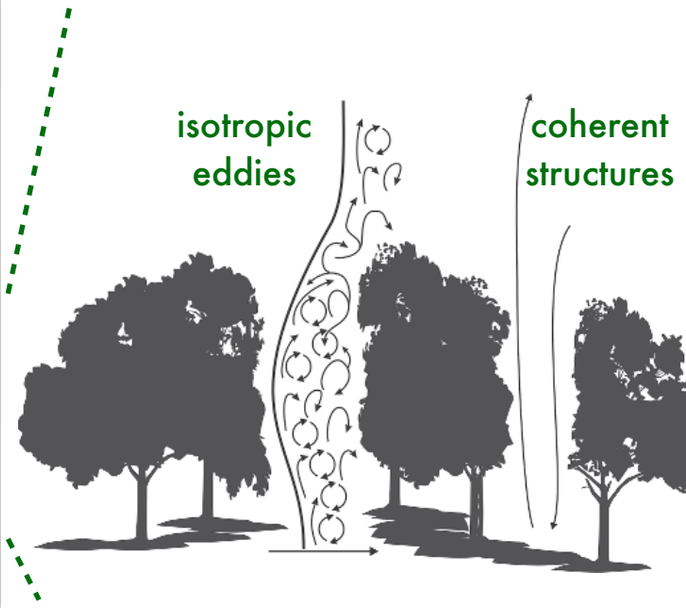

Structure of the Planetary Boundary Layer

Idealised PBL

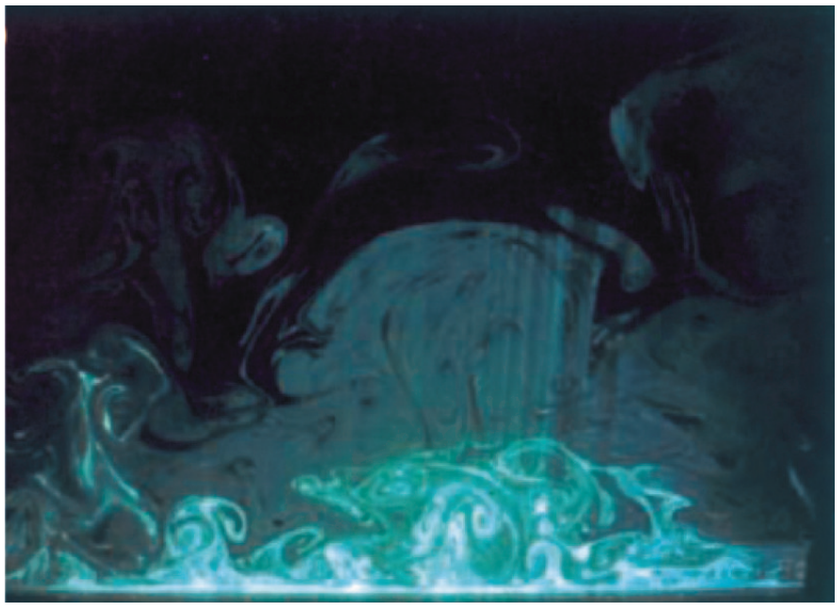

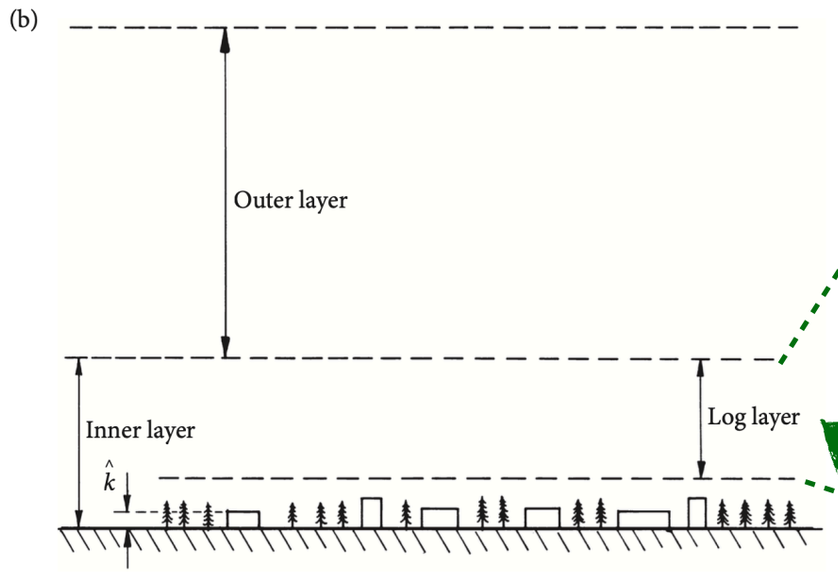

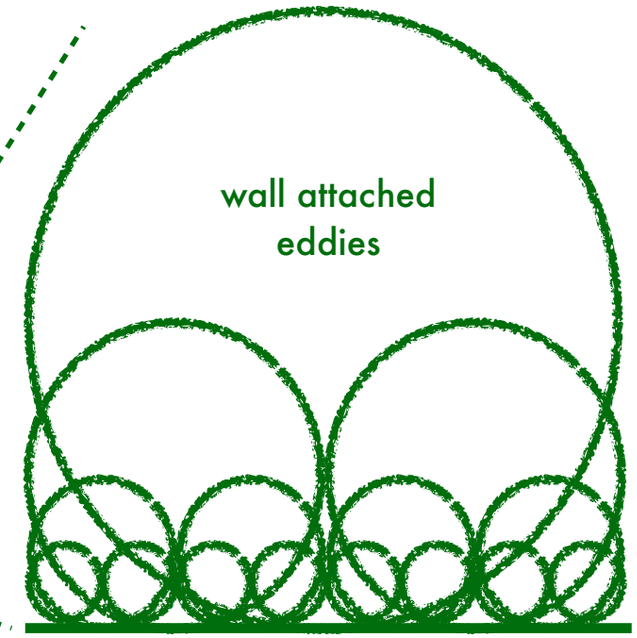

Real PBL

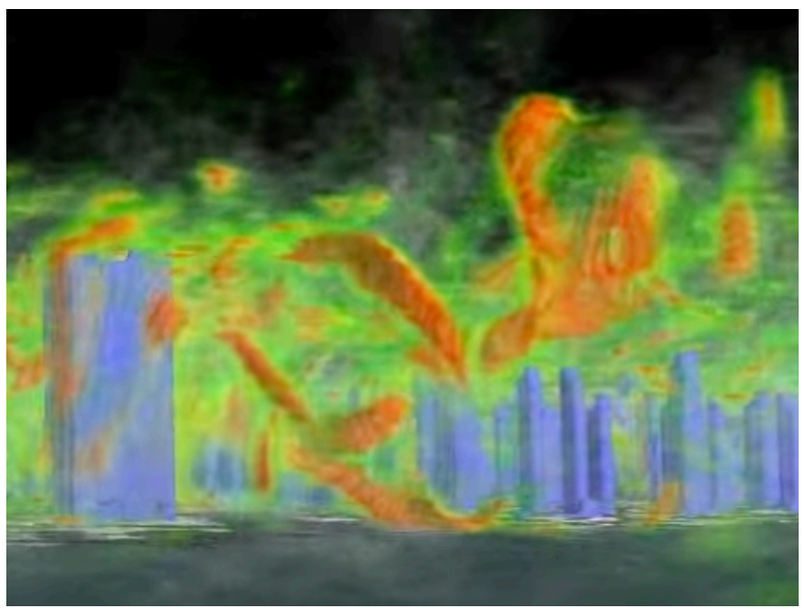

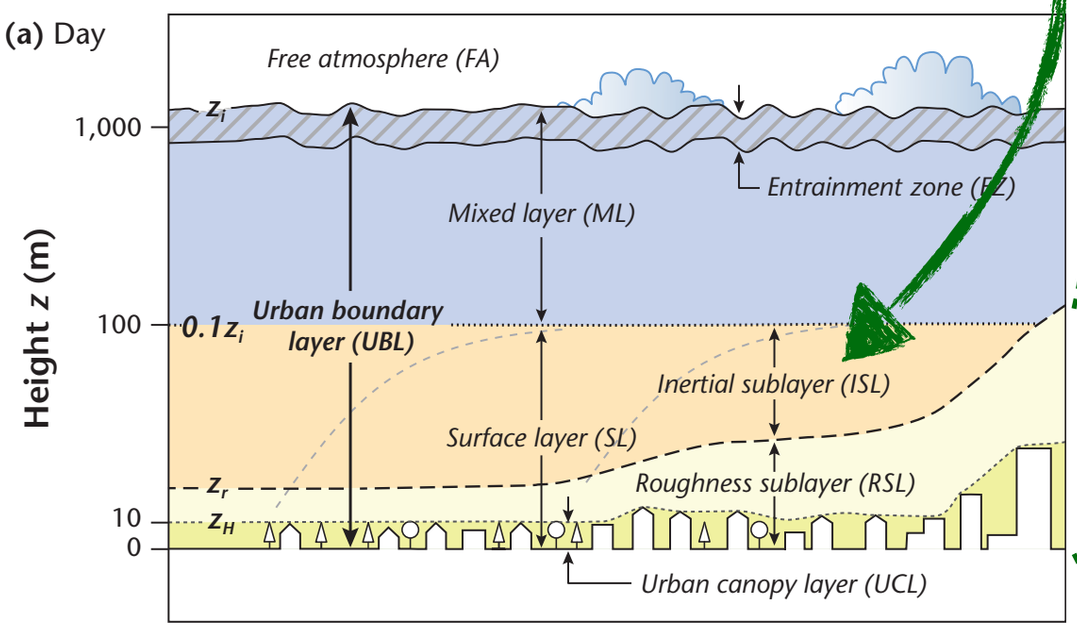

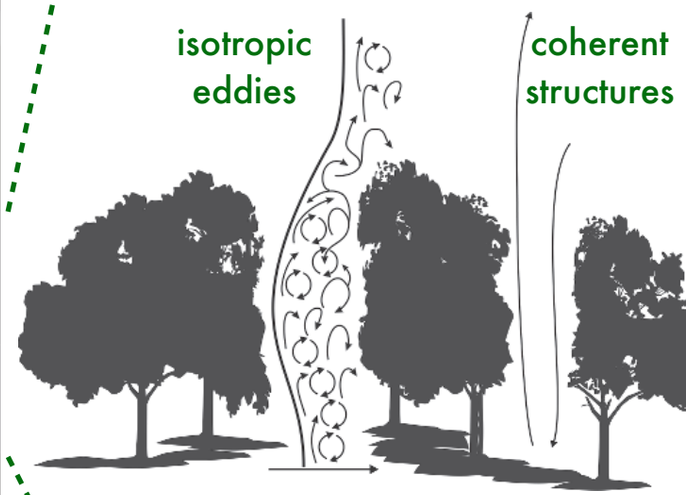

The Roughness Sublayer

The RSL significance to a plethora of physical, chemical, and biological processes is not in dispute. It suffices to note that Earth Systems and Numerical Weather Predictions models require a handshake between the land surface and the atmosphere.

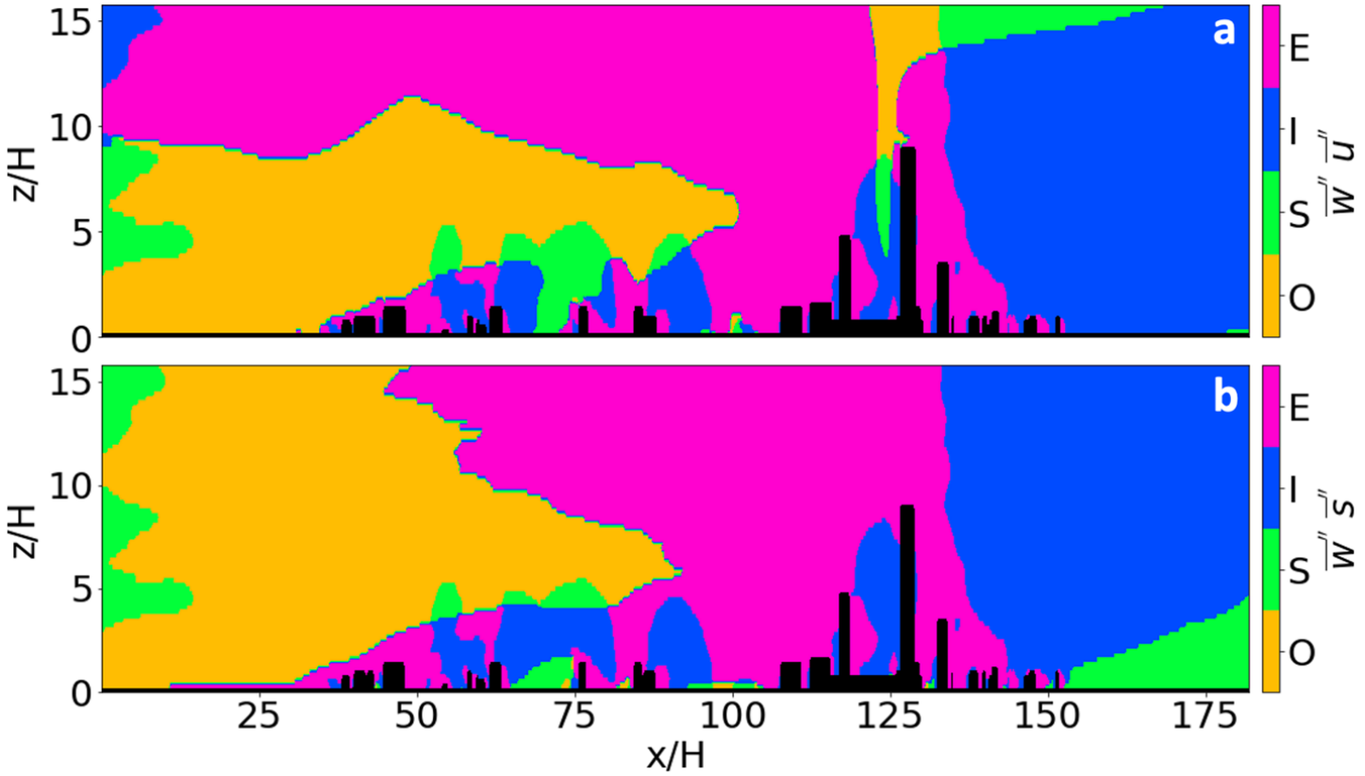

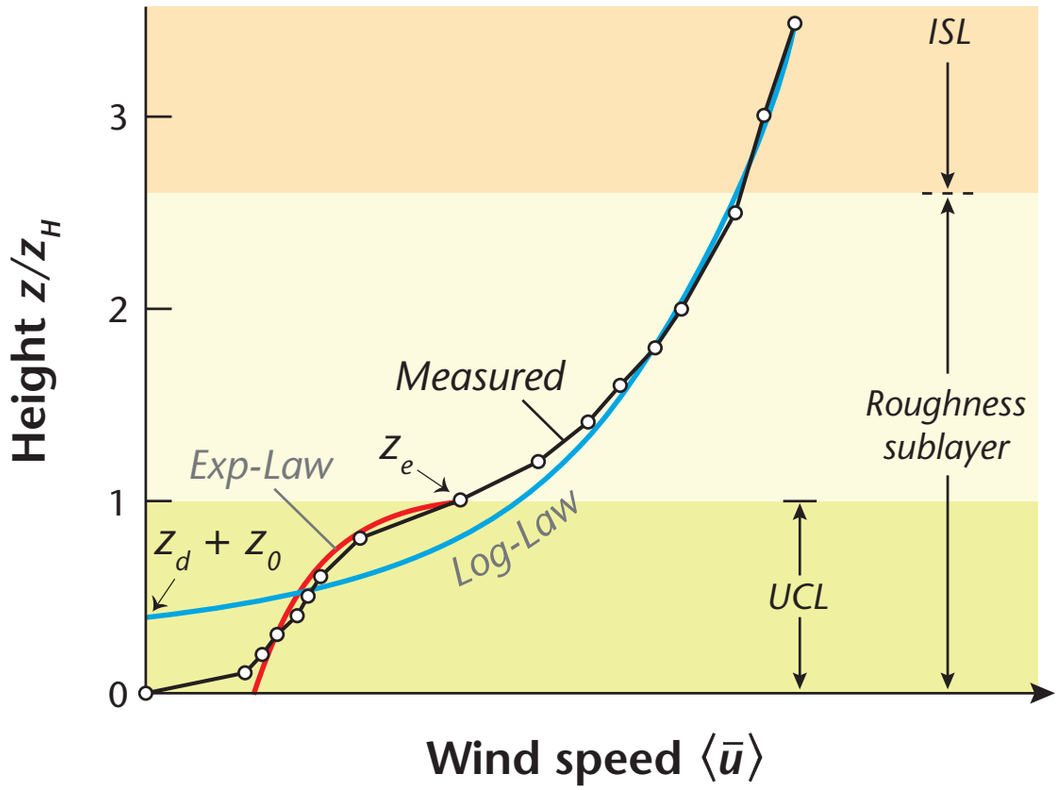

In spite of its crucial role in land-Atmosphere exchange processes, even for homogeneous canopies there are still unanswered questions at a fundamental level that prevent the understanding and the modelling of turbulent flows in the RSL.

Oke et al. (2017), Akinlabi et al. (2022)

Mixing Layer Analogy

Raupach, Finnigan and Brunet (1996)

Fully developed turbulence

Boundary Layer

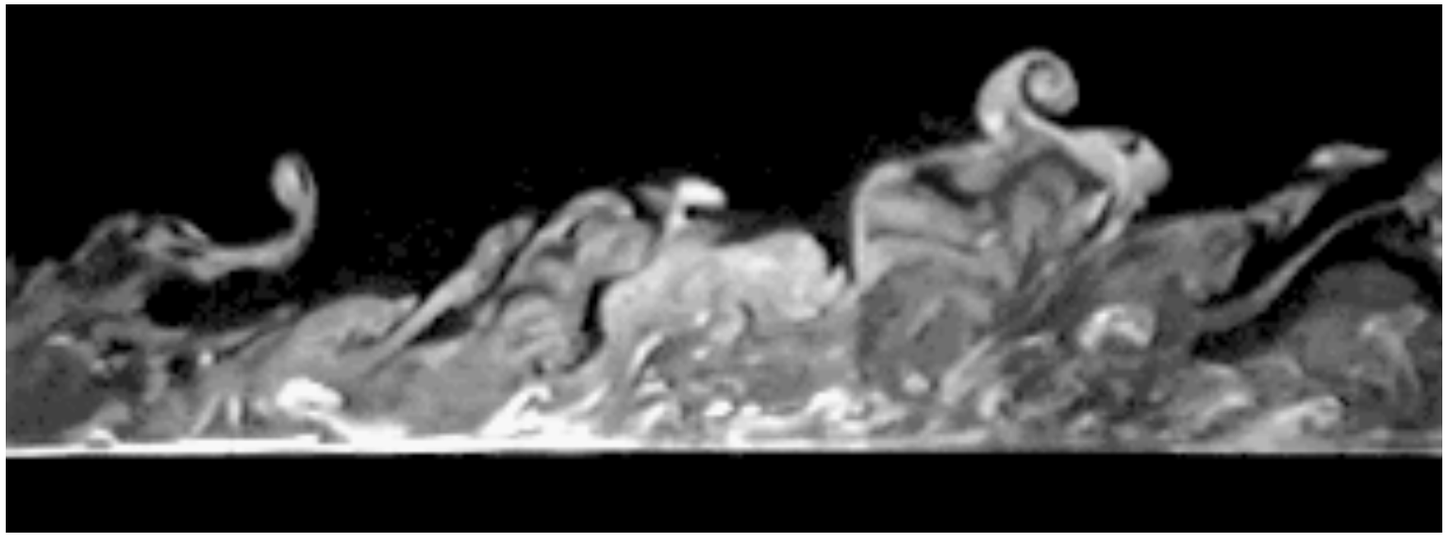

$U(z)$

Old eddies with longer straining time

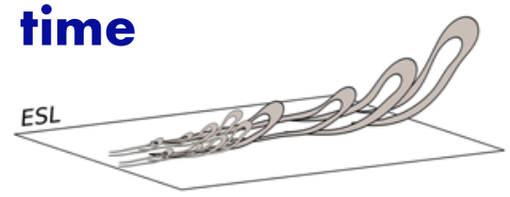

$$L_{BL} = \kappa_v (z - d)$$

Mixing Layer Analogy

Raupach, Finnigan and Brunet (1996)

Fully developed turbulence

Boundary Layer

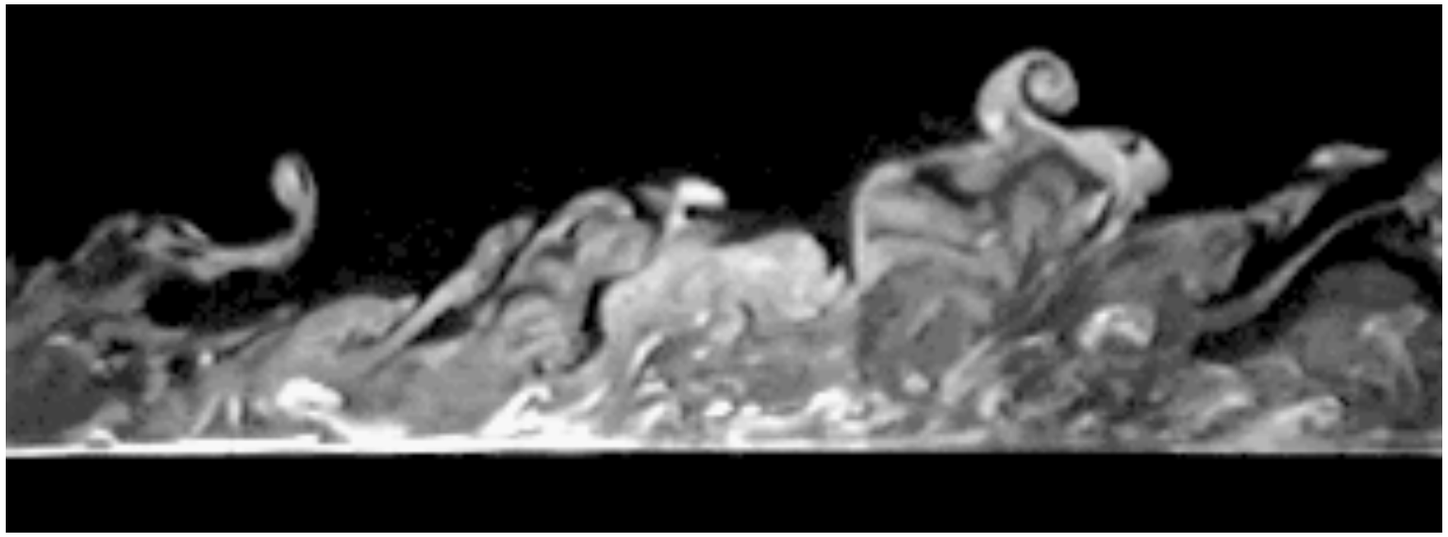

$U(z)$

Old eddies with longer straining time

$$L_{BL} = \kappa_v (z - d)$$

Coherent Structure

Mixing Layer
Van Dyke (1982)

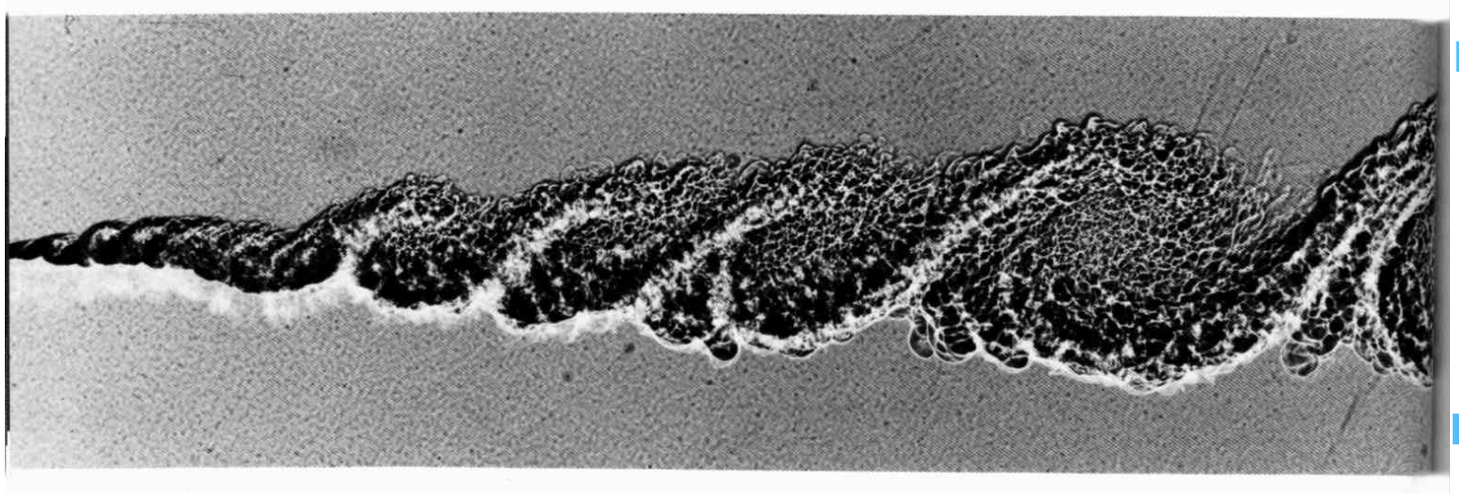

$U(z)$

Young eddies

$$L_S = U(h) / \frac{dU}{dz}$$

Mixing Layer Analogy

Raupach, Finnigan and Brunet (1996)

Fully developed turbulence

Boundary Layer

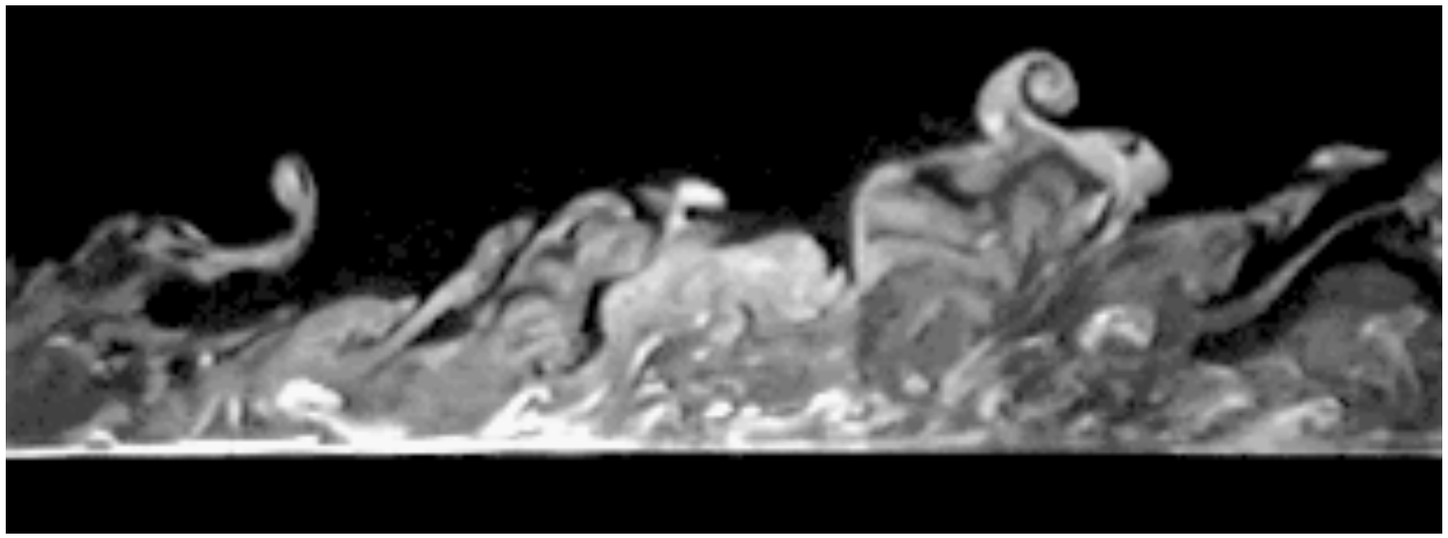

$U(z)$

Old eddies with longer straining time

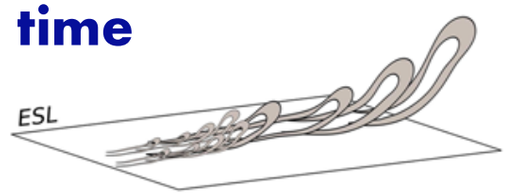

$$L_{BL} = \kappa_v (z - d)$$

Coherent Structure

Mixing Layer
Van Dyke (1982)

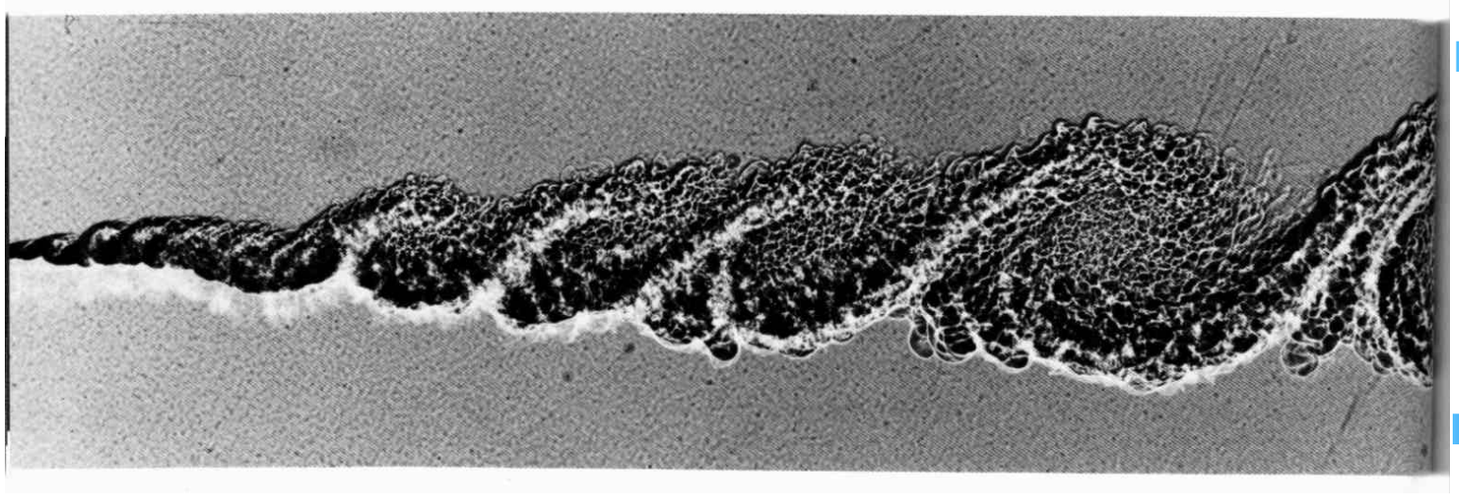

$U(z)$

Young eddies

$$L_S = U(h) / \frac{dU}{dz}$$

Unfortunately, this approach cannot be applied to urban canopies, since turbulent length scales become relatively small at the canopy top and are not dominated by large scale eddies generated by shear instabilities at the inflection point of the wind profile.

A new perspective for the Roughness Sublayer: the Cospectral Budget Model

The idea is to describe the Roughness Sublayer starting from the energetics of turbulence whereby all eddy sizes contribute to momentum transport.

As a matter of facts, while conventional mixing length theories attribute a single mixing length to momentum transport, Roughness sublayer turbulence involves multiple length scales prompting interest in how to accommodate all of them in the estimation of appropriate stability functions.

The law-of-the wall.
Departures from the logarithmic profile

Assuming that the law-of-the wall (i.e. a logarithmic profile) holds in the Inertial Sublayer, the RSL effects can be accommodated through a correction function:

$$\frac{\kappa_v(z-d)}{u_*}\frac{dU}{dz} = \phi_{RSL}\left(z/z_*, d/h, \dots\right)$$

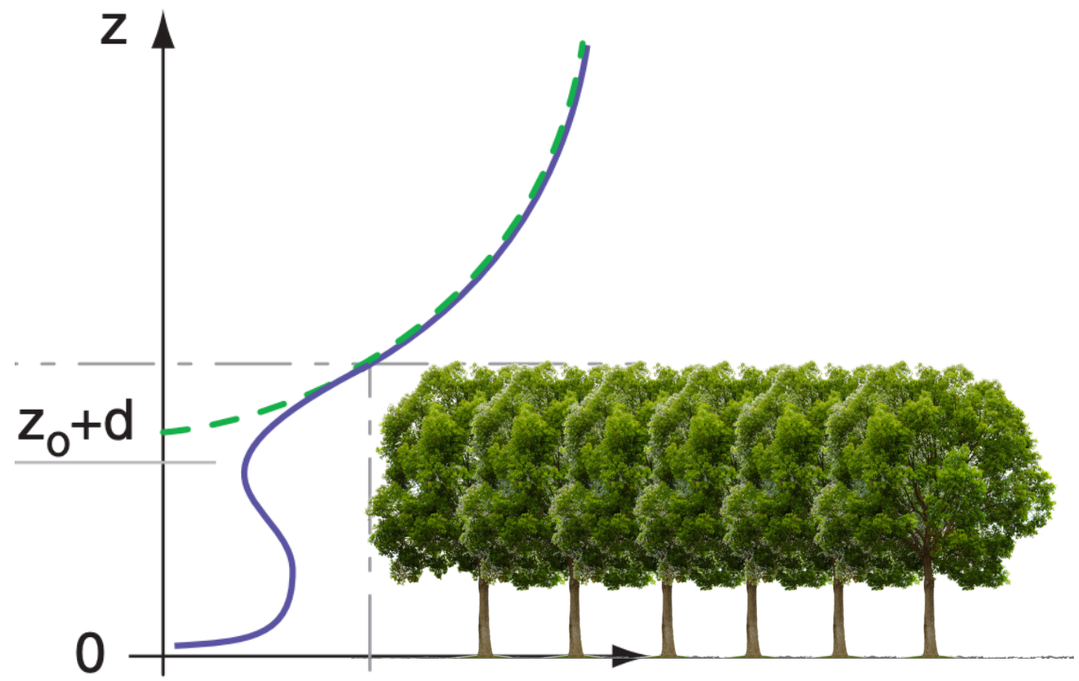

By virtue of this definition, the log-law is recovered when $\phi_{RSL}(\,.\,) = 1$ though more significant is its independence of z. For this reason, phenomenological theories describing $\phi_{RSL}(\,.\,)$ assume that $\phi_{RSL}(\,.\,) \to 1$ when $z \to \infty$.

$$\frac{\kappa_v(z-d)}{u_*}\frac{dU}{dz} = 1 \quad \longrightarrow \quad U(z) = \frac{u_*}{\kappa_v}\, log\frac{z-d}{z_0}$$

Thus, $\phi_{RSL}(\,.\,)$ is a dimensionless roughness sublayer modification function yet to be determined and frames the scope of the work here for near-neutral conditions.

The law-of-the wall.
Departures from the logarithmic profile

Laboratory and field studies suggest enhancement in momentum transport in the RSL when compared to ISL predictions, thereby requiring that: $\phi_{RSL} \leq 1$

Empirical form

$$\phi_{RSL} = 1 - \exp\left[-a_1\left(\frac{z-d}{z_*}\right)\right]$$

→ empirical

Mixing Layer Analogy

(Raupach et al., 1996; Harman and Finnigan, 2007)

$$\frac{\kappa_v(z-d)}{u_*}\frac{dU}{dz} = \hat{\phi}_{RSL}\left(\frac{z+d_t}{\delta_\omega}\right)$$

→ These descriptions associate a single (and fastest) growing mode of instability (Kelvin-Helmholtz type) leading to coherent structures to be the dominant effective mixing-length ignoring all other energetic modes in the spectrum of turbulence that contribute to momentum fluxes.

The law-of-the wall.
Departures from the logarithmic profile

Laboratory and field studies suggest enhancement in momentum transport in the RSL when compared to ISL predictions, thereby requiring that: $\phi_{RSL} \leq 1$

Empirical form

$$\phi_{RSL} = 1 - \exp\left[-a_1\left(\frac{z-d}{z_*}\right)\right]$$

→ empirical

Mixing Layer Analogy

(Raupach et al., 1996; Harman and Finnigan, 2007)

$$\frac{\kappa_v(z-d)}{u_*}\frac{dU}{dz} = \hat{\phi}_{RSL}\left(\frac{z+d_t}{\delta_\omega}\right)$$

→ These descriptions associate a single (and fastest) growing mode of instability (Kelvin-Helmholtz type) leading to coherent structures to be the dominant effective mixing-length ignoring all other energetic modes in the spectrum of turbulence that contribute to momentum fluxes.

What appears missing is a connection between $\phi_{RSL}(\,.\,)$ and the turbulent fluctuations carried by eddies of all sizes

The law-of-the wall.
Departures from the logarithmic profile

Laboratory and field studies suggest enhancement in momentum transport in the RSL when compared to ISL predictions, thereby requiring that: $\phi_{RSL} \leq 1$

Empirical form

$$\phi_{RSL} = 1 - \exp\left[-a_1\left(\frac{z-d}{z_*}\right)\right]$$

→ empirical

Mixing Layer Analogy

(Raupach et al., 1996; Harman and Finnigan, 2007)

$$\frac{\kappa_v(z-d)}{u_*}\frac{dU}{dz} = \hat{\phi}_{RSL}\left(\frac{z+d_t}{\delta_\omega}\right)$$

→ These descriptions associate a single (and fastest) growing mode of instability (Kelvin-Helmholtz type) leading to coherent structures to be the dominant effective mixing-length ignoring all other energetic modes in the spectrum of turbulence that contribute to momentum fluxes.

What appears missing is a connection between $\phi_{RSL}(\,.\,)$ and the turbulent fluctuations carried by eddies of all sizes

RSL turbulence involves multiple length scales prompting interest in how to accommodate all of them in the estimation of ϕ_{RSL}. The work here seeks to arrive at a description of ϕ_{RSL} starting from the energetics of turbulence whereby all eddy sizes contribute to momentum transport.

Moving Equilibrium Hypothesis

Stationary, Homogeneous ISL, $Re_d \to \infty$

Moving Equilibrium Hypothesis

Stationary, Homogeneous ISL, $Re_d \to \infty$

- mean vertical momentum balance: $\dfrac{\partial \sigma_w^2}{\partial z} = -\dfrac{1}{\overline{\rho}}\dfrac{\partial \overline{P}}{\partial z} - g$

Moving Equilibrium Hypothesis

Stationary, Homogeneous ISL, $Re_d \to \infty$

- mean vertical momentum balance: $\dfrac{\partial \sigma_w^2}{\partial z} = -\dfrac{1}{\overline{\rho}}\dfrac{\partial \overline{P}}{\partial z} - g$

- mean longitudinal momentum balance: $\dfrac{\partial \overline{w'u'}}{\partial z} = -\dfrac{1}{\overline{\rho}}\dfrac{\partial \overline{P}}{\partial x}$

Moving Equilibrium Hypothesis

Stationary, Homogeneous ISL, $Re_d \to \infty$

- mean vertical momentum balance: $\dfrac{\partial \sigma_w^2}{\partial z} = -\dfrac{1}{\overline{\rho}}\dfrac{\partial \overline{P}}{\partial z} - g$
- mean longitudinal momentum balance: $\dfrac{\partial \overline{w'u'}}{\partial z} = -\dfrac{1}{\overline{\rho}}\dfrac{\partial \overline{P}}{\partial x}$
- turbulent kinetic energy balance: $P_m = -\overline{u'w'}\dfrac{dU}{dz} = \epsilon$

Moving Equilibrium Hypothesis

Stationary, Homogeneous ISL, $Re_d \to \infty$

- mean vertical momentum balance: $\frac{\partial \sigma_w^2}{\partial z} = -\frac{1}{\overline{\rho}}\frac{\partial \overline{P}}{\partial z} - g$ → (near-neutral ISL) $\frac{\partial \sigma_w^2}{\partial z} = 0$

- mean longitudinal momentum balance: $\frac{\partial \overline{w'u'}}{\partial z} = -\frac{1}{\overline{\rho}}\frac{\partial \overline{P}}{\partial x}$ → (MOST) $\frac{\partial \overline{w'u'}}{\partial z} = 0$

- turbulent kinetic energy balance: $P_m = -\overline{u'w'}\frac{dU}{dz} = \epsilon$

Moving Equilibrium Hypothesis

Stationary, Homogeneous ISL, $Re_d \to \infty$

Contrary to many agricultural sites, forests are rarely situated on uniform and flat terrain.

- mean vertical momentum balance: $\dfrac{\partial \sigma_w^2}{\partial z} = -\dfrac{1}{\overline{\rho}}\dfrac{\partial \overline{P}}{\partial z} - g$

- mean longitudinal momentum balance: $\dfrac{\partial \overline{w'u'}}{\partial z} = -\dfrac{1}{\overline{\rho}}\dfrac{\partial \overline{P}}{\partial x}$

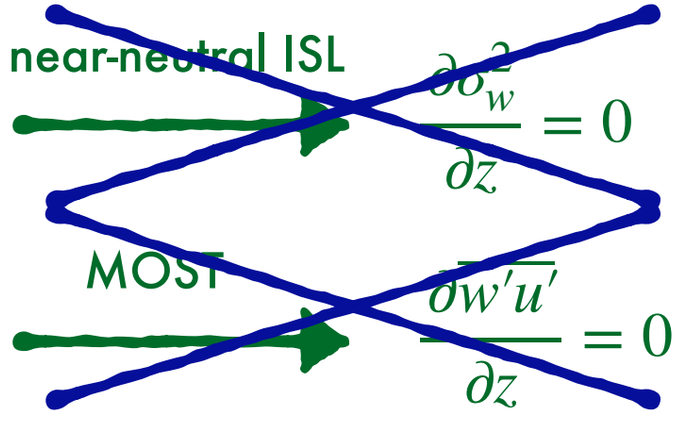

- turbulent kinetic energy balance: $P_m = -\overline{u'w'}\dfrac{dU}{dz} = \epsilon$

In the absence of a mean longitudinal pressure gradient, $\overline{u'w'} = -u_*^2$ and is independent of z. Its value may be set at $z/h = 1$. Measured deviations from a constant σ_w^2 and $\overline{u'w'}$ with z may signify modifications to $\overline{P}$ expected over non-flat terrain.

Moving Equilibrium Hypothesis

Stationary, Homogeneous ISL, $Re_d \to \infty$

Contrary to many agricultural sites, forests are rarely situated on uniform and flat terrain.

- mean vertical momentum balance: $\dfrac{\partial \sigma_w^2}{\partial z} = -\dfrac{1}{\overline{\rho}}\dfrac{\partial \overline{P}}{\partial z} - g$

- mean longitudinal momentum balance: $\dfrac{\partial \overline{w'u'}}{\partial z} = -\dfrac{1}{\overline{\rho}}\dfrac{\partial \overline{P}}{\partial x}$

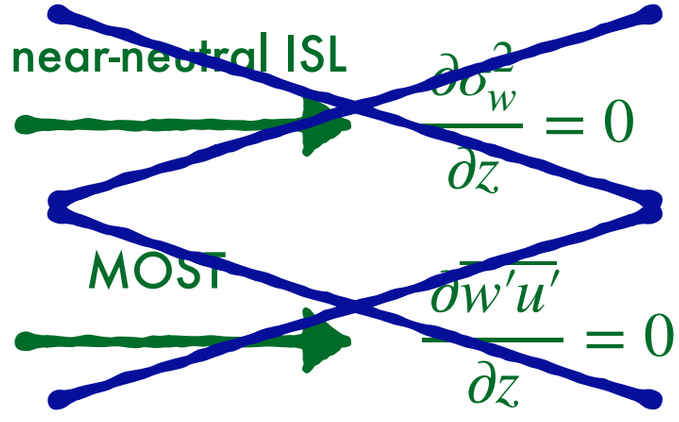

- turbulent kinetic energy balance: $P_m = -\overline{u'w'}\dfrac{dU}{dz} = \epsilon$

In the absence of a mean longitudinal pressure gradient, $\overline{u'w'} = -u_*^2$ and is independent of z. Its value may be set at $z/h = 1$. Measured deviations from a constant σ_w^2 and $\overline{u'w'}$ with z may signify modifications to $\overline{P}$ expected over non-flat terrain.

Provided these modifications to $\overline{P}$ are not too large to introduce mean advective terms, the assumptions of stationary and planar homogeneous flow conditions in the absence of subsidence may still hold in the ISL though the independence of stresses and σ_w^2 from z may not. This is the essence of the moving equilibrium hypothesis (Kader and Yaglom, 1978, Yaglom, 1979)

Model 1:
A stress budget model

In stationary and planar homogeneous high Reynolds number flow and in the absence of subsidence, the turbulent stress budget reduces to

$$\frac{\partial \overline{u'w'}}{\partial t} = 0 = -\sigma_w^2 \frac{dU}{dz} - \frac{\partial \overline{w'w'u'}}{\partial z} + R_{u,w} - 2\epsilon_{uw},$$

Model 1:
A stress budget model

In stationary and planar homogeneous high Reynolds number flow and in the absence of subsidence, the turbulent stress budget reduces to

$$\frac{\partial \overline{u'w'}}{\partial t} = 0 = -\sigma_w^2 \frac{dU}{dz} - \frac{\partial \overline{w'w'u'}}{\partial z} + R_{u,w} - 2\epsilon_{uw},$$

flux transport

viscous de-correlation

mechanical production

pressure rate of strain de-correlation

Model 1:
A stress budget model

In stationary and planar homogeneous high Reynolds number flow and in the absence of subsidence, the turbulent stress budget reduces to

flux transport

viscous de-correlation

$$\frac{\partial \overline{u'w'}}{\partial t} = 0 = -\sigma_w^2 \frac{dU}{dz} - \frac{\partial \overline{w'w'u'}}{\partial z} + R_{u,w} - 2\nu \overline{u_{i,j}w_{i,j}},$$

mechanical production

pressure rate of strain de-correlation

Model 1:
A stress budget model

In stationary and planar homogeneous high Reynolds number flow and in the absence of subsidence, the turbulent stress budget reduces to

flux transport

viscous de-correlation

$$\frac{\partial \overline{u'w'}}{\partial t} = 0 = -\sigma_w^2 \frac{dU}{dz} - \frac{\partial \overline{w'w'u'}}{\partial z} + R_{u,w} - 2\nu \overline{u'w'},$$

mechanical production

pressure rate of strain de-correlation

$R_{u,w}$ can be parameterised using the LRR-PI model (Rotta return-to-isotropy closure scheme corrected for the isotropization of the production):

$$-(1 - C_I)\sigma_w^2 \frac{dU}{dz} - C_R \frac{\overline{w'u'}}{\tau} = 0$$

Model 1:
A stress budget model

In stationary and planar homogeneous high Reynolds number flow and in the absence of subsidence, the turbulent stress budget reduces to

flux transport

$$\frac{\partial \overline{u'w'}}{\partial t} = 0 = -\sigma_w^2 \frac{dU}{dz} - \frac{\partial \overline{w'w'u'}}{\partial z} + R_{u,w} - 2\epsilon_{u,w},$$

viscous de-correlation

mechanical production

pressure rate of strain de-correlation

$R_{u,w}$ can be parameterised using the LRR-PI model (Rotta return-to-isotropy closure scheme corrected for the isotropization of the production):

$$-(1 - C_I)\sigma_w^2 \frac{dU}{dz} - C_R \frac{\overline{w'u'}}{\tau} = 0$$

$C_R = 1.8,\ C_I = 0.6$

$A = \dfrac{C_R}{1 - C_I} = 4.5$

de-correlation timescale $\tau = \dfrac{2\sigma_w^2}{\epsilon}$

Model 1:
A stress budget model

In stationary and planar homogeneous high Reynolds number flow and in the absence of subsidence, the turbulent stress budget reduces to

flux transport

$$\frac{\partial \overline{u'w'}}{\partial t} = 0 = -\sigma_w^2 \frac{dU}{dz} - \frac{\partial \overline{w'w'u'}}{\partial z} + R_{u,w} - 2\epsilon_{u,w},$$

viscous de-correlation

mechanical production

pressure rate of strain de-correlation

$R_{u,w}$ can be parameterised using the LRR-PI model (Rotta return-to-isotropy closure scheme corrected for the isotropization of the production):

$$-(1 - C_I)\sigma_w^2 \frac{dU}{dz} - C_R \frac{\overline{w'u'}}{\tau} = 0$$

$C_R = 1.8,\ C_I = 0.6$

$A = \dfrac{C_R}{1 - C_I} = 4.5$

de-correlation timescale $\tau = \dfrac{2\sigma_w^2}{\epsilon}$

$$-\frac{1}{A}\frac{\tau\sigma_w^2}{\overline{u'w'}}\frac{dU}{dz} = 1$$

Model 1:
A stress budget model

In stationary and planar homogeneous high Reynolds number flow and in the absence of subsidence, the turbulent stress budget reduces to

flux transport

$$\frac{\partial \overline{u'w'}}{\partial t} = 0 = -\sigma_w^2 \frac{dU}{dz} - \frac{\partial \overline{w'w'u'}}{\partial z} + R_{u,w} - 2\epsilon_{u,w},$$

viscous de-correlation

mechanical production

pressure rate of strain de-correlation

$R_{u,w}$ can be parameterised using the LRR-PI model (Rotta return-to-isotropy closure scheme corrected for the isotropization of the production):

$$-(1 - C_I)\sigma_w^2 \frac{dU}{dz} - C_R \frac{\overline{w'u'}}{\tau} = 0$$

$C_R = 1.8,\ C_I = 0.6$

$A = \dfrac{C_R}{1 - C_I} = 4.5$

de-correlation timescale $\tau = \dfrac{2\sigma_w^2}{\epsilon}$

$$-\frac{1}{A}\frac{\tau\sigma_w^2}{\overline{u'w'}}\frac{dU}{dz} = 1 \quad \rightarrow \quad \phi_{RSL} = -A\frac{\overline{u'w'}}{u_*^2}\frac{u_*}{\sigma_w}\frac{L_{BL}}{\tau\sigma_w}$$

Model 1:
A stress budget model

$$\phi_{RSL} = \frac{L_{BL}}{u_*}\frac{dU}{dz} \longrightarrow \phi_{RSL} = -A\frac{\overline{u'w'}}{u_*^2}\frac{u_*}{\sigma_w}\frac{L_{BL}}{\tau\sigma_w}$$

Model 1 shows that suggests that the RSL introduces deviations from $\phi_{RSL} = 1$ through 2 key mechanisms:

- an $\overline{u'w'}/u_*^2$ and σ_w/u_* dependency on z presumably due to presence of **complex topography** distorting $\overline{P}$ from its idealized ISL budget expectations

- a $\tau\sigma_w$that no longer scales with $L_{BL} = \kappa_v(z-d)$.

Model 1:
A stress budget model

$$\phi_{RSL} = \frac{L_{BL}}{u_*}\frac{dU}{dz} \longrightarrow \phi_{RSL} = -A\frac{\overline{u'w'}}{u_*^2}\frac{u_*}{\sigma_w}\frac{L_{BL}}{\tau\sigma_w}$$

Model 1 shows that suggests that the RSL introduces deviations from $\phi_{RSL} = 1$ through 2 key mechanisms:

- an $\overline{u'w'}/u_*^2$ and σ_w/u_* dependency on z presumably due to presence of **complex topography** distorting $\overline{P}$ from its idealized ISL budget expectations

- a $\tau\sigma_w$ that no longer scales with $L_{BL} = \kappa_v(z-d)$. $\tau = \frac{2\sigma_w^2}{\epsilon}$

Model 1 $$\phi_{RSL} = -\frac{A}{2}\frac{\overline{u'w'}}{u_*^2}\left(\frac{u_*}{\sigma_w}\right)^4\frac{L_{BL}}{L_d}$$

Model 1:
A stress budget model

$$\phi_{RSL} = \frac{L_{BL}}{u_*}\frac{dU}{dz} \quad \longrightarrow \quad \phi_{RSL} = -A\frac{\overline{u'w'}}{u_*^2}\frac{u_*}{\sigma_w}\frac{L_{BL}}{\tau\sigma_w}$$

Model 1 shows that suggests that the RSL introduces deviations from $\phi_{RSL} = 1$ through 2 key mechanisms:

- an $\overline{u'w'}/u_*^2$ and σ_w/u_* dependency on z presumably due to presence of **complex topography** distorting $\overline{P}$ from its idealized ISL budget expectations

- a $\tau\sigma_w$ that no longer scales with $L_{BL} = \kappa_v(z-d)$. $\tau = \frac{2\sigma_w^2}{\epsilon}$

Model 1 $$\phi_{RSL} = -\frac{A}{2}\frac{\overline{u'w'}}{u_*^2}\left(\frac{u_*}{\sigma_w}\right)^4\frac{L_{BL}}{L_d}$$

$L_d = \frac{u_*^3}{\epsilon(z)}$ is the dissipation length scale (an integral scale much larger than the Kolmogorov microscale:

$$Re_d = \frac{u_* L_d}{\nu} \quad \longrightarrow \quad \frac{L_d}{\eta} = Re_d^{3/4}$$

Model 2:
A Cospectral Budget Model

Model 2 is a scale wise extension of Model 1.

The presence of an RSL is expected to distort the vertical velocity spectrum, $E_{ww}(k)$, from its 'canonical' shape in the ISL. Since

$$\sigma_w^2 = \int_0^\infty E_{ww}(k)dk$$

These distortions can then be translated to ϕ_{RSL} estimates at various heights above the canopy through a co-spectral budget (CSB) model.

Model 2:
A Cospectral Budget Model

Model 2 is a scale wise extension of Model 1.

The presence of an RSL is expected to distort the vertical velocity spectrum, $E_{ww}(k)$, from its 'canonical' shape in the ISL. Since

$$\sigma_w^2 = \int_0^\infty E_{ww}(k)dk$$

These distortions can then be translated to ϕ_{RSL} estimates at various heights above the canopy through a co-spectral budget (CSB) model.

Katul et al. (2013) CSB model for homogeneous turbulence is

$$\frac{\partial F_{wu}(k)}{\partial t} + 2\nu k^2 F_{wu}(k) = P_{wu}(k) + T_{wu}(k) + \pi(k)$$

Model 2:
A Cospectral Budget Model

Model 2 is a scale wise extension of Model 1.

The presence of an RSL is expected to distort the vertical velocity spectrum, $E_{ww}(k)$, from its 'canonical' shape in the ISL. Since

$$\sigma_w^2 = \int_0^\infty E_{ww}(k)dk$$

These distortions can then be translated to ϕ_{RSL} estimates at various heights above the canopy through a co-spectral budget (CSB) model.

Katul et al. (2013) CSB model for homogeneous turbulence is

$$\epsilon_{wu} = 2\nu \int_0^\infty k^2 F_{wu}(k)dk \qquad P_{wu}(k) = -\frac{dU}{dz} E_{ww}(k)$$

$$\frac{\partial F_{wu}(k)}{\partial t} + 2\nu k^2 F_{wu}(k) = P_{wu}(k) + T_{wu}(k) + \pi(k)$$

co-spectral flux transfer

velocity - pressure interaction term

Model 2:
A Cospectral Budget Model

Model 2 is a scale wise extension of Model 1.

The presence of an RSL is expected to distort the vertical velocity spectrum, $E_{ww}(k)$, from its 'canonical' shape in the ISL. Since

$$\sigma_w^2 = \int_0^\infty E_{ww}(k)dk$$

These distortions can then be translated to ϕ_{RSL} estimates at various heights above the canopy through a co-spectral budget (CSB) model.

Katul et al. (2013) CSB model for homogeneous turbulence is

$$\epsilon_{wu} = 2\nu \int_0^\infty k^2 F_{wu}(k)dk \qquad P_{wu}(k) = -\frac{dU}{dz}E_{ww}(k)$$

$$\cancel{\frac{\partial F_{wu}(k)}{\partial t}} + 2\nu k^2 F_{wu}(k) = P_{wu}(k) + \cancel{T_{wu}(k)} + \pi(k)$$

co-spectral flux transfer

velocity - pressure interaction term

Model 2:
A Cospectral Budget Model

Model 2 is a scale wise extension of Model 1.

The presence of an RSL is expected to distort the vertical velocity spectrum, $E_{ww}(k)$, from its 'canonical' shape in the ISL. Since

$$\sigma_w^2 = \int_0^\infty E_{ww}(k)dk$$

These distortions can then be translated to ϕ_{RSL} estimates at various heights above the canopy through a co-spectral budget (CSB) model.

Katul et al. (2013) CSB model for homogeneous turbulence is

$$\epsilon_{wu} = 2\nu \int_0^\infty k^2 F_{wu}(k)dk \qquad P_{wu}(k) = -\frac{dU}{dz}E_{ww}(k)$$

$$\frac{\partial F_{wu}(k)}{\partial t} + 2\nu k^2 F_{wu}(k) = P_{wu}(k) + T_{wu}(k) + \pi(k)$$

co-spectral flux transfer

velocity - pressure interaction term

A scale-wise closure a scale-wise isotropization of the production term that corrects the original Rotta scheme is used for $\pi(k)$ to give:

$$(1 - C_I)\frac{dU}{dz}E_{ww}(k) - \frac{C_R}{\tau(k)}F_{wu}(k) = 2\nu k^2 F_{wu}(k)\,.$$

Model 2:
A Cospectral Budget Model

Model 2 is a scale wise extension of Model 1.

The presence of an RSL is expected to distort the vertical velocity spectrum, $E_{ww}(k)$, from its 'canonical' shape in the ISL. Since

$$\sigma_w^2 = \int_0^\infty E_{ww}(k)dk$$

These distortions can then be translated to ϕ_{RSL} estimates at various heights above the canopy through a co-spectral budget (CSB) model.

Katul et al. (2013) CSB model for homogeneous turbulence is

$$\epsilon_{wu} = 2\nu \int_0^\infty k^2 F_{wu}(k)dk \qquad P_{wu}(k) = -\frac{dU}{dz}E_{ww}(k)$$

$$\frac{\partial F_{wu}(k)}{\partial t} + 2\nu k^2 F_{wu}(k) = P_{wu}(k) + T_{wu}(k) + \pi(k)$$

co-spectral flux transfer

velocity - pressure interaction term

A scale-wise closure a scale-wise isotropization of the production term that corrects the original Rotta scheme is used for $\pi(k)$ to give:

$$(1 - C_I)\frac{dU}{dz}E_{ww}(k) - \frac{C_R}{\tau(k)}F_{wu}(k) = 2\nu k^2 F_{wu}(k)\,.$$

Model 2:
A Cospectral Budget Model

$$-\frac{1}{A}\frac{\tau\sigma_w^2}{\overline{w'u'}}\frac{dU}{dz} = 1 \qquad -F_{wu}(k) = A^{-1}\frac{dU}{dz}\tau(k)E_{ww}(k)$$

$\tau(k) = \alpha\epsilon^{-1/3}k^{-2/3}$ relaxation time at k associated with turbulent stress de-correlation

Model 2:
A Cospectral Budget Model

$$-\frac{1}{A}\frac{\tau\sigma_w^2}{\overline{w'u'}}\frac{dU}{dz} = 1 \qquad -F_{wu}(k) = A^{-1}\frac{dU}{dz}\tau(k)E_{ww}(k)$$

$\tau(k) = \alpha\epsilon^{-1/3}k^{-2/3}$ relaxation time at k associated with turbulent stress de-correlation

Integrating over k and remembering that $\phi_{RSL} = \dfrac{\kappa_v(z-d)}{u_*}\dfrac{dU}{dz}$ we have

Model 2 $$\phi_{RSL} = -A\left(\frac{\overline{u'w'}}{u_*^2}\right)\left(\frac{u_*\, L_{BL}}{\int_0^\infty \tau(k)E_{ww}(k)dk}\right)$$

Distortions to the scale-wise product $\tau(k)E_{ww}(k)$ by the RSL away from their canonical ISL shapes can now be directly linked to deviations of ϕ_{RSL} from unity.

Model 2:
A Cospectral Budget Model

$$-\frac{1}{A}\frac{\tau\sigma_w^2}{\overline{w'u'}}\frac{dU}{dz} = 1 \qquad -F_{wu}(k) = A^{-1}\frac{dU}{dz}\tau(k)E_{ww}(k)$$

$\tau(k) = \alpha\epsilon^{-1/3}k^{-2/3}$ relaxation time at k associated with turbulent stress de-correlation

Integrating over k and remembering that $\phi_{RSL} = \dfrac{\kappa_v(z-d)}{u_*}\dfrac{dU}{dz}$ we have

Model 2 $$\phi_{RSL} = -A\left(\frac{\overline{u'w'}}{u_*^2}\right)\left(\frac{u_*\, L_{BL}}{\int_0^\infty \tau(k)E_{ww}(k)dk}\right)$$

Distortions to the scale-wise product $\tau(k)E_{ww}(k)$ by the RSL away from their canonical ISL shapes can now be directly linked to deviations of ϕ_{RSL} from unity.

As a side result, The CSB model unambiguously shows that the appropriate eddy viscosity, ν_t, that applies simultaneously in the RSL and ISL is given by

$$\nu_t = \frac{1-C_I}{C_R}\int_0^\infty \tau(k)E_{ww}(k)dk$$

Model 3:
A Simplified Cospectral Budget Model

The idea behind Model 3 is to prescribe an idealised behaviour for $E_{ww}(k)$

$$\phi_{RSL} = -A\left(\frac{\overline{u'w'}}{u_*^2}\right)\left(\frac{u_*\ L_{BL}}{\int_0^\infty \tau(k)E_{ww}(k)dk}\right)$$

Model 3:
A Simplified Cospectral Budget Model

The idea behind Model 3 is to prescribe an idealised behaviour for $E_{ww}(k)$

$$\phi_{RSL} = -A\left(\frac{\overline{u'w'}}{u_*^2}\right)\left(\frac{u_*\, L_{BL}}{\int_0^\infty \tau(k) E_{ww}(k)\, dk}\right)$$

- An inertial subrange region (ISR) is expected at high wavenumbers where $E_{ww}(k) \sim k^{-5/3}$.

Model 3:
A Simplified Cospectral Budget Model

The idea behind Model 3 is to prescribe an idealised behaviour for $E_{ww}(k)$

$$\phi_{RSL} = -A\left(\frac{\overline{u'w'}}{u_*^2}\right)\left(\frac{u_*\, L_{BL}}{\int_0^\infty \tau(k) E_{ww}(k)\, dk}\right)$$

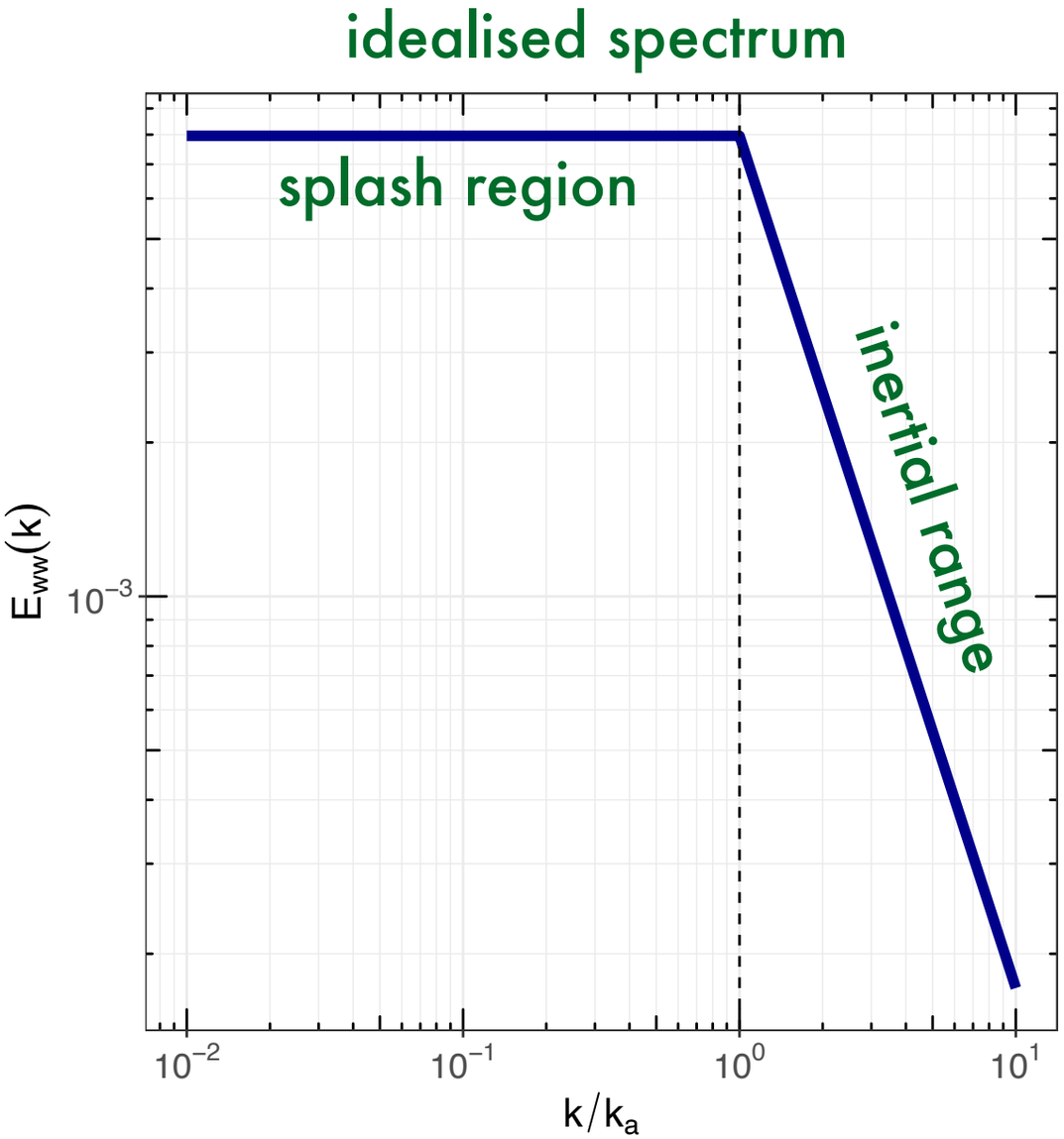

- An inertial subrange region (ISR) is expected at high wavenumbers where $E_{ww}(k) \sim k^{-5/3}$.

- At large scales, the $E_{ww}(k)$ may be characterized by an energy-splashing region (i.e. $E_{ww}(k) \sim k^{0}$).

Model 3:
A Simplified Cospectral Budget Model

The idea behind Model 3 is to prescribe an idealised behaviour for $E_{ww}(k)$

$$\phi_{RSL} = -A\left(\frac{\overline{u'w'}}{u_*^2}\right)\left(\frac{u_*\, L_{BL}}{\int_0^\infty \tau(k) E_{ww}(k) dk}\right)$$

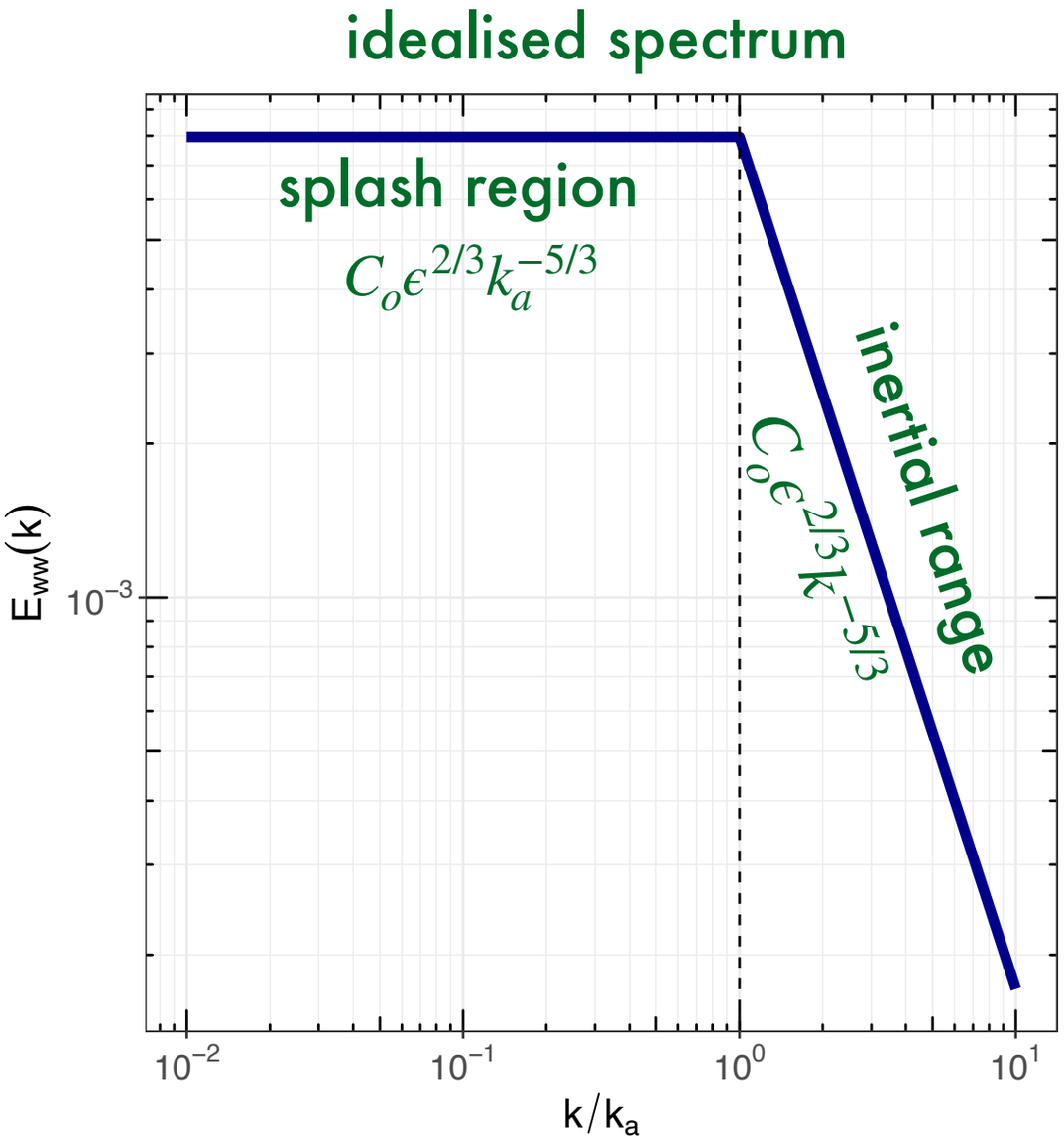

- An inertial subrange region (ISR) is expected at high wavenumbers where $E_{ww}(k) \sim k^{-5/3}$.

- At large scales, the $E_{ww}(k)$ may be characterized by an energy-splashing region (i.e. $E_{ww}(k) \sim k^0$).

- A model of maximum simplicity is to introduce a transition wavenumber between them designated by k_a.

$$E_{ww}(k) = \begin{cases} C_o\epsilon^{2/3}k_a^{-5/3} & \forall k/k_a \leq 1 \\ C_o\epsilon^{2/3}k^{-5/3} & \forall k/k_a > 1 \end{cases}$$

Model 3:
A Simplified Cospectral Budget Model

Model 3 $$\phi_{RSL} = -\frac{5}{3}\frac{AC_o}{\alpha}\left(\frac{\overline{u'w'}}{u_*^2}\right)\left(\frac{u_*}{\sigma_w}\right)^4\frac{L_{BL}}{L_d}$$

As in Model 1, the ratio $\frac{L_{BL}}{L_d}$ shows how a lack in equilibrium in the tke balance ($P_m/\epsilon \neq 1$) can impact ϕ_{RSL} through the dissipation length scale L_d.

Model 3:
A Simplified Cospectral Budget Model

Model 3 $$\phi_{RSL} = -\frac{5}{3}\frac{AC_o}{\alpha}\left(\frac{\overline{u'w'}}{u_*^2}\right)\left(\frac{u_*}{\sigma_w}\right)^4\frac{L_{BL}}{L_d}$$

As in Model 1, the ratio $\frac{L_{BL}}{L_d}$ shows how a lack in equilibrium in the tke balance ($P_m/\epsilon \neq 1$) can impact ϕ_{RSL} through the dissipation length scale L_d.

$$\phi_{RSL} = \begin{cases} -\frac{A}{2}\frac{\overline{u'w'}}{u_*^2}\left(\frac{u_*}{\sigma_w}\right)^4\frac{L_{BL}}{L_d} \\ -A\left(\frac{\overline{u'w'}}{u_*^2}\right)\left(\frac{u_*\ L_{BL}}{\int_0^\infty \tau(k)E_{ww}(k)dk}\right) \\ -\frac{5}{3}\frac{AC_o}{\alpha}\left(\frac{\overline{u'w'}}{u_*^2}\right)\left(\frac{u_*}{\sigma_w}\right)^4\frac{L_{BL}}{L_d} \end{cases}$$

- Model 2 and 3 are identical if the experimental $E_{ww}(k)$ spectra follow the idealised behaviour.
- Model 1 and 3 become identical when setting $\alpha = \frac{10}{3}C_o$ in the formulation of $\tau(k)$

The Amazon Tall Tower Observatory

The ATTO site is situated in the central Amazon rainforest of Brazil, in a pristine area, up till now mostly unaffected by deforestation or other human interference. In fact, it is situated within the Uatumã Sustainable Development Reserve. This ensures that it will remain undisturbed for some years to come.

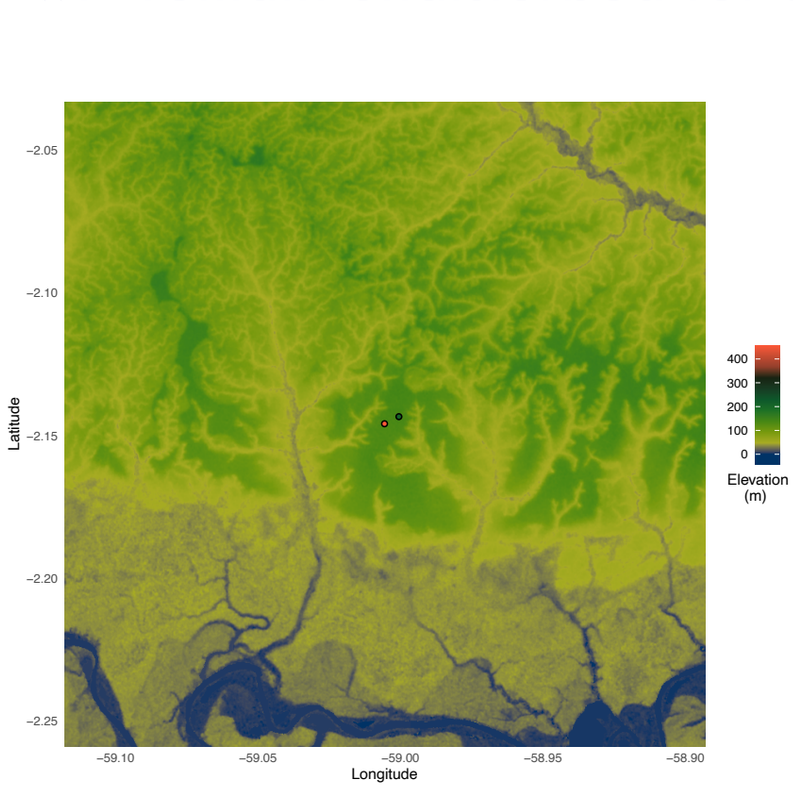

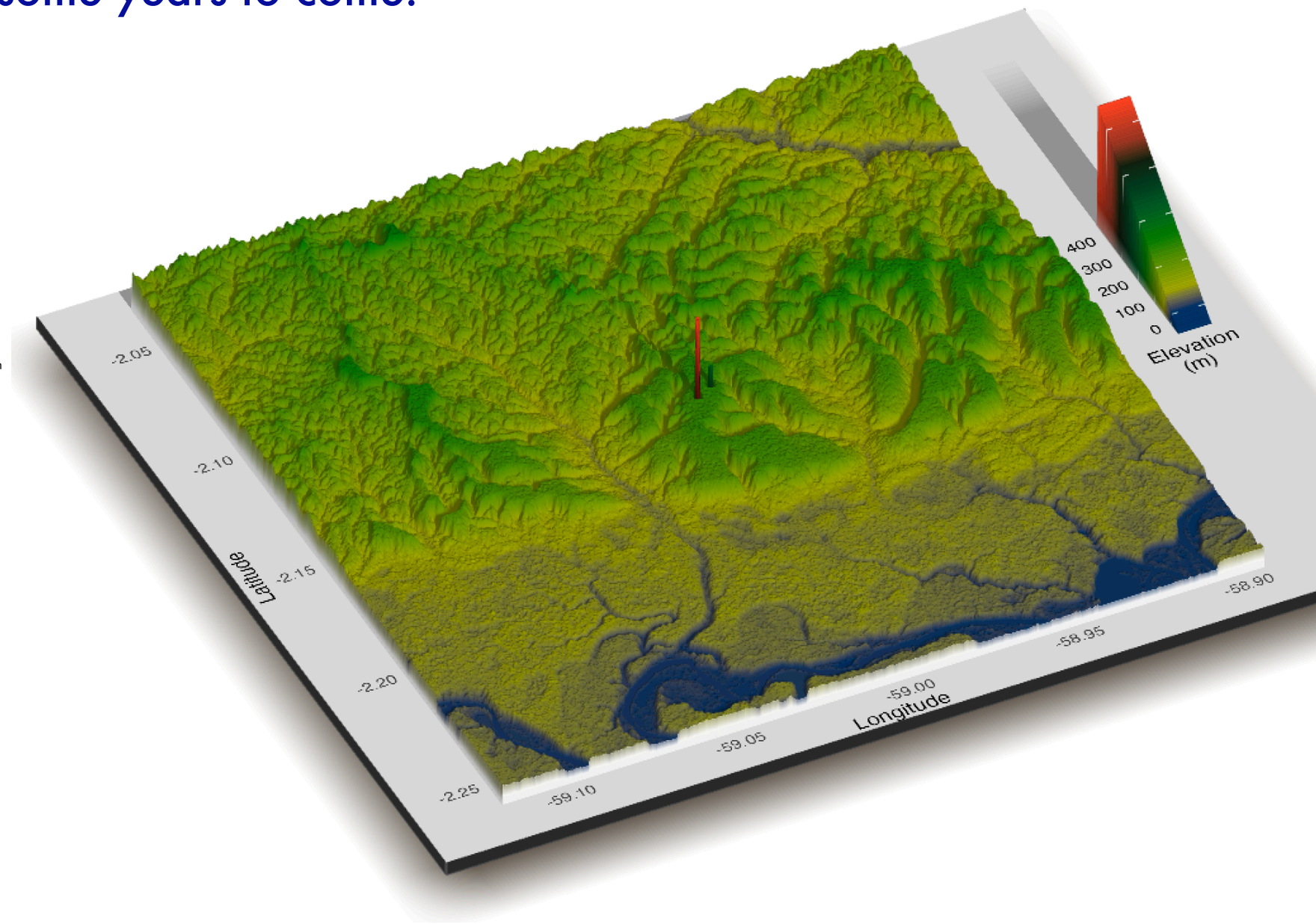

ATTO
AMAZON TALL TOWER OBSERVATORY

www.attoproject.org

The Amazon Tall Tower Observatory

IOP Campaign 2015

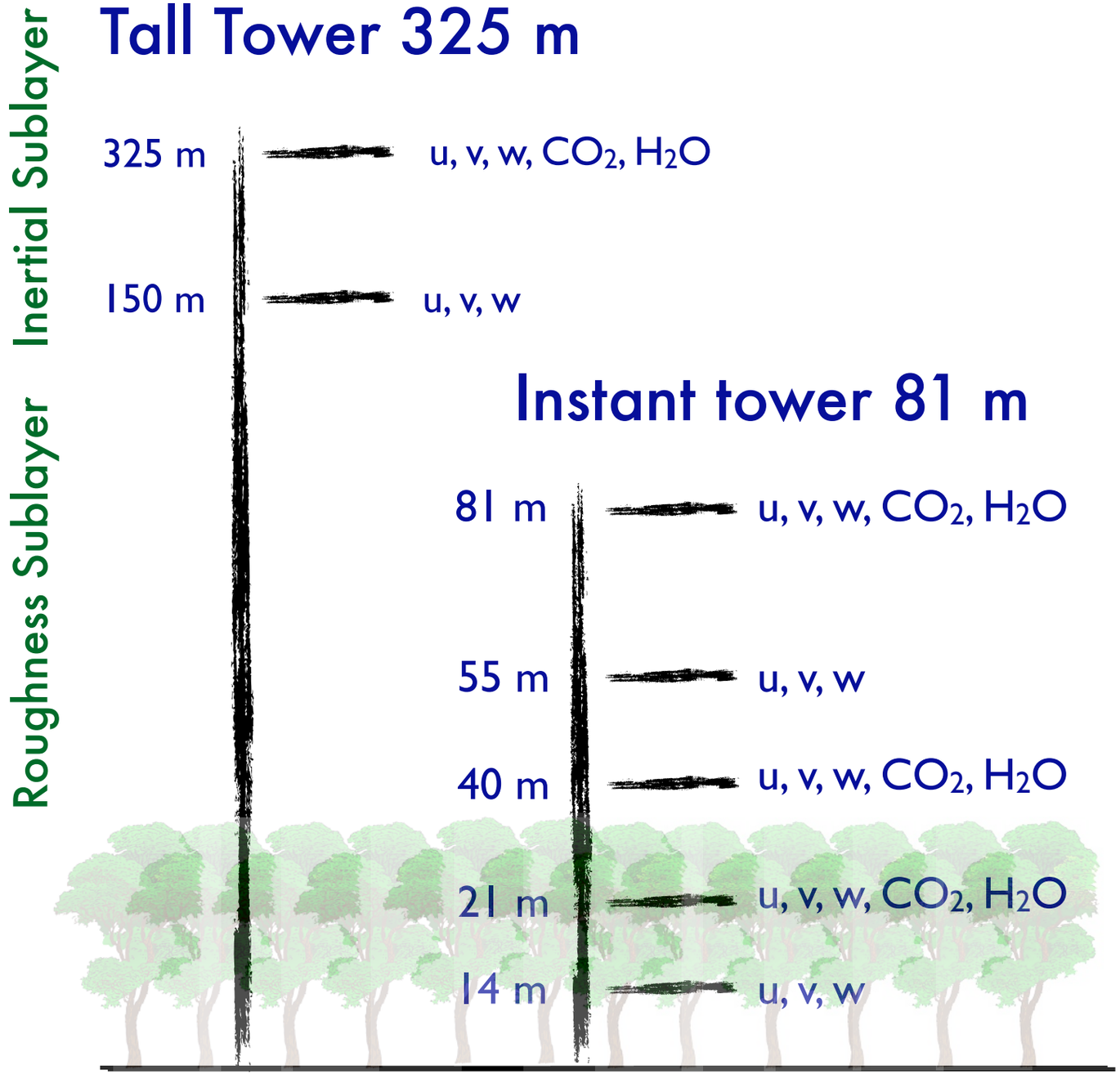

The Amazon Tall Tower Observatory

IOP Campaign 2015

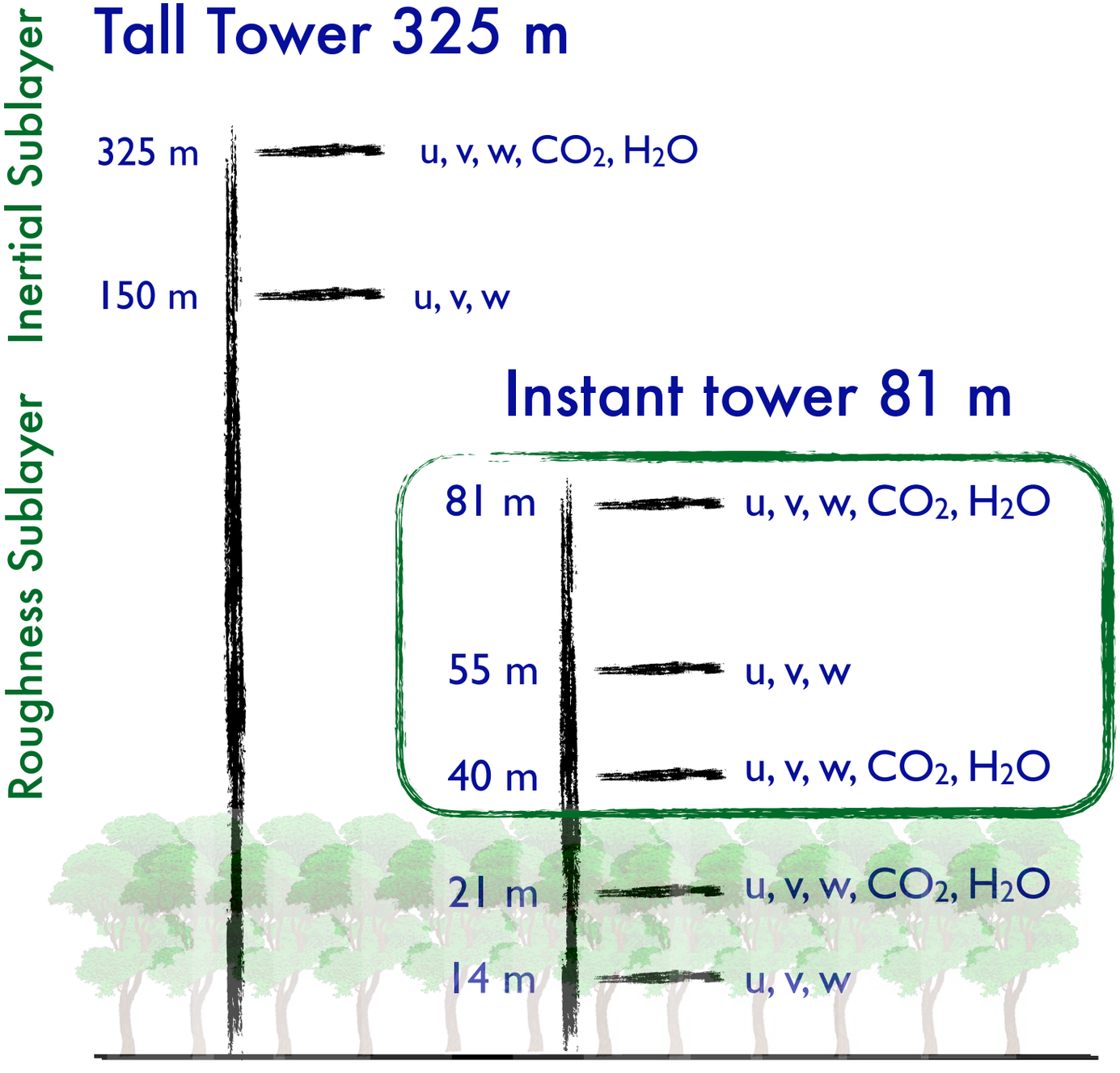

Results: bulk flow statistics

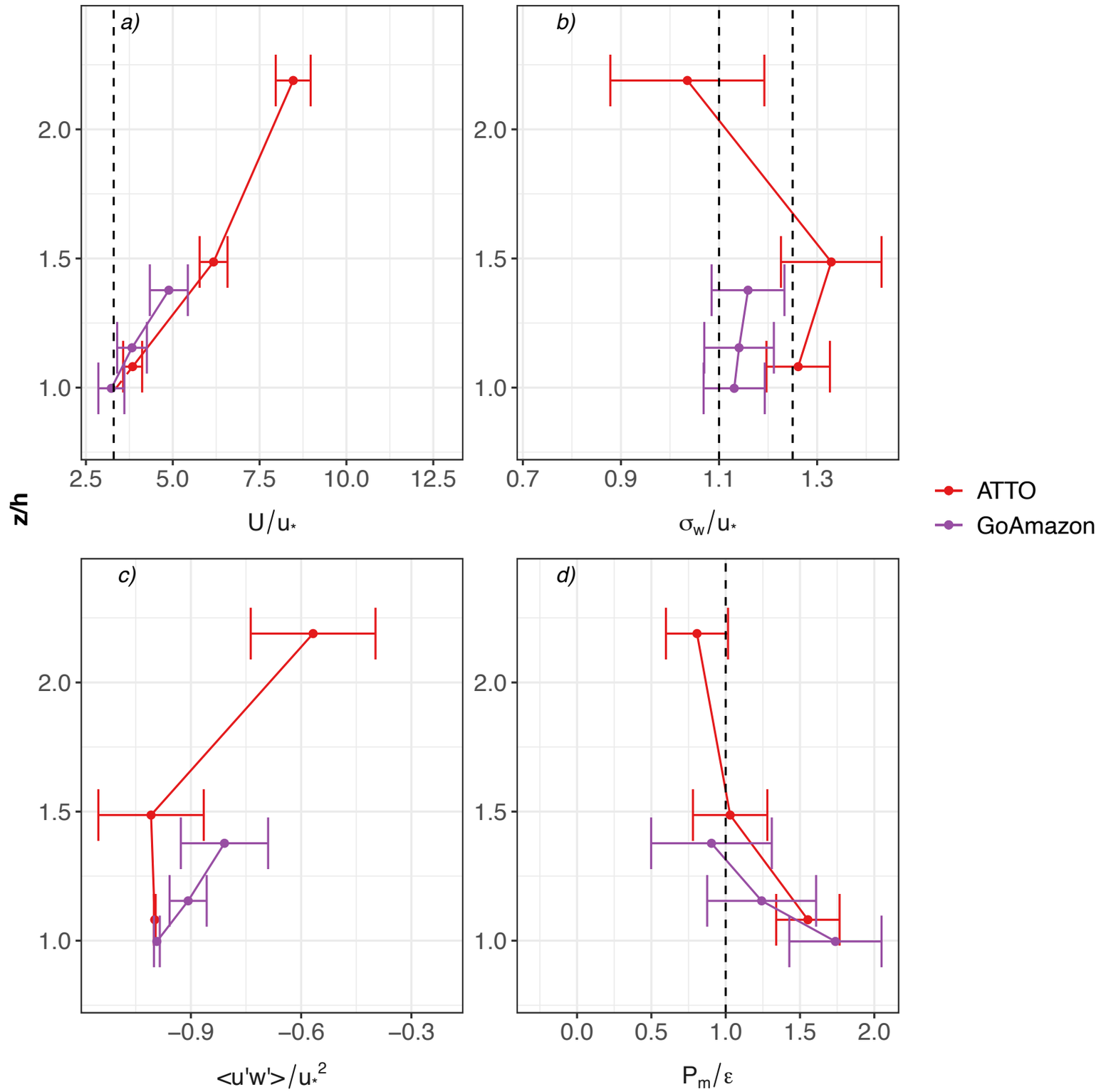

Results: bulk flow statistics

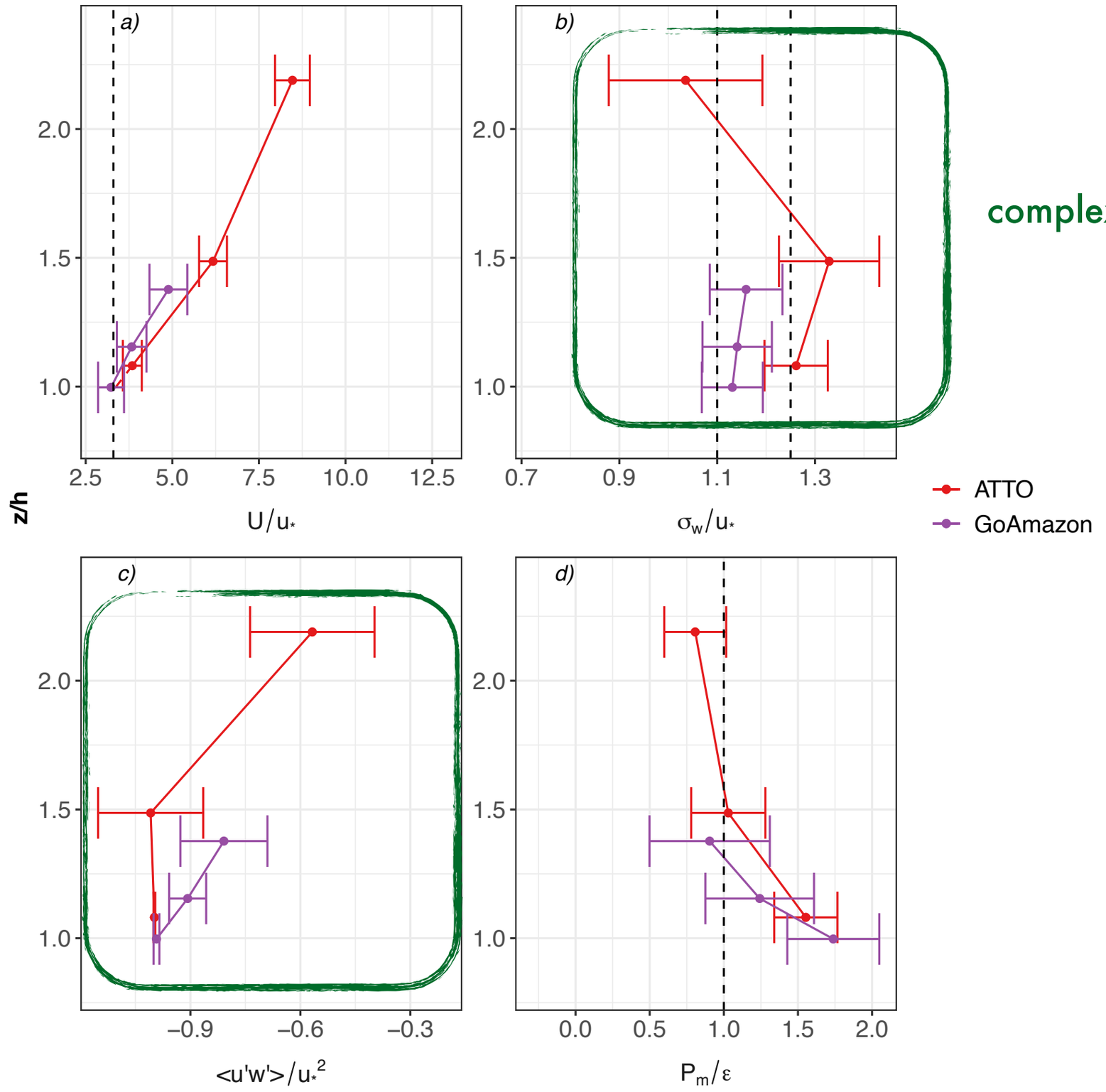

complex terrain

complex terrain

Results: bulk flow statistics

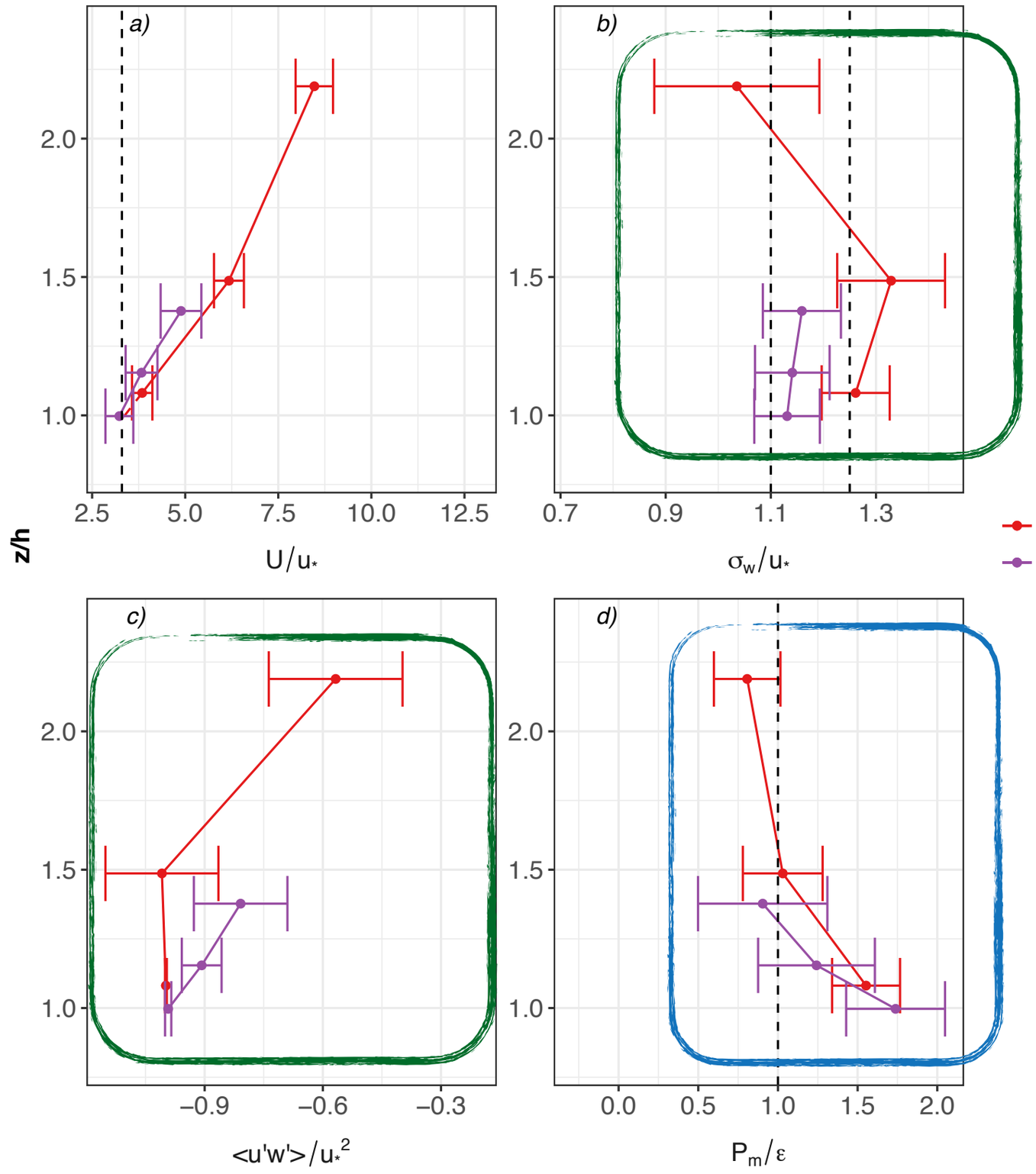

complex terrain

complex terrain

$$\frac{P_m}{\epsilon} \neq 1$$

Results: Spectral and Cospectral Properties

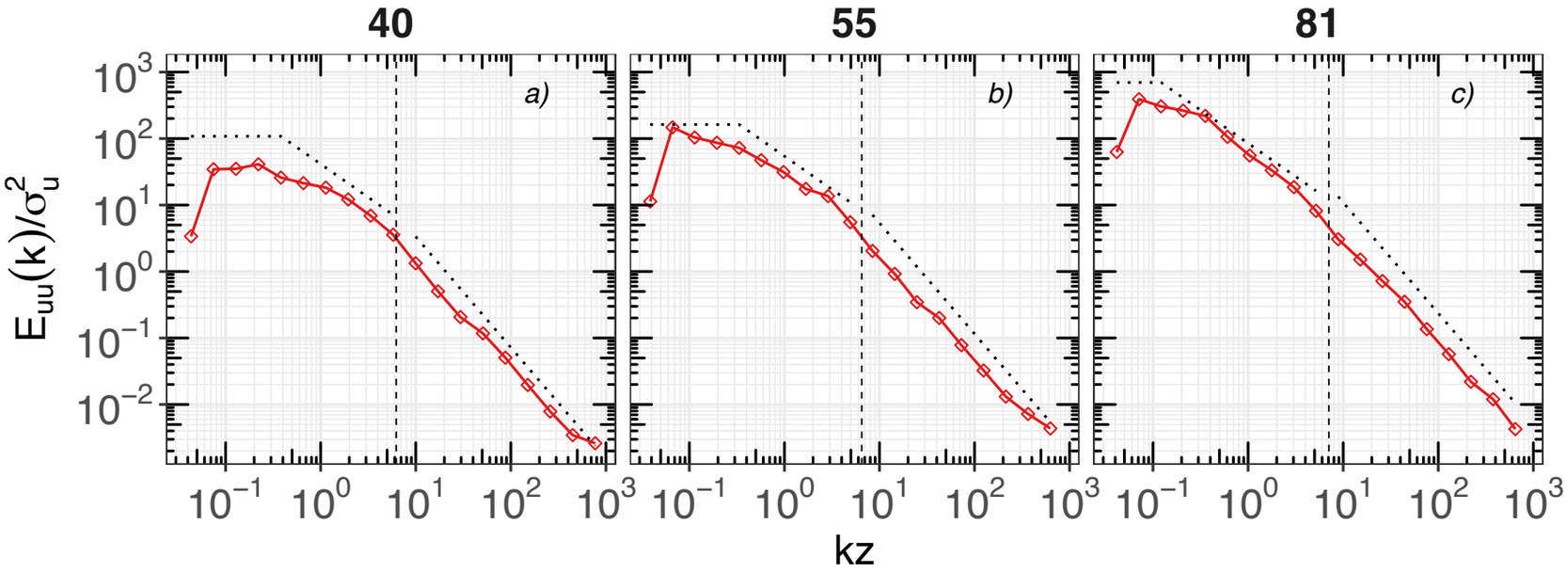

$E_{uu}(k)$ exhibits an extended ISR scaling at all levels for smaller eddies ($kz > 1$). As z/h increases and the influence of RSL turbulence weakens, the onset of a k^{-1} scaling becomes evident at low wavenumbers ($kz < 1$) suggestive of dominance of attached eddies.

$E_{ww}(k)$ also exhibits an extended ISR scaling for $kz > 1$ at all z. At $kz < 1$, the emerging picture is rather different. Near the canopy top, the measured $E_{ww}(k)$ is well approximated by the idealized shape. With increasing z/h, deviations from a flat energy-splashing region at $kz < 1$ become noticeable.

Results: Spectral and Cospectral Properties

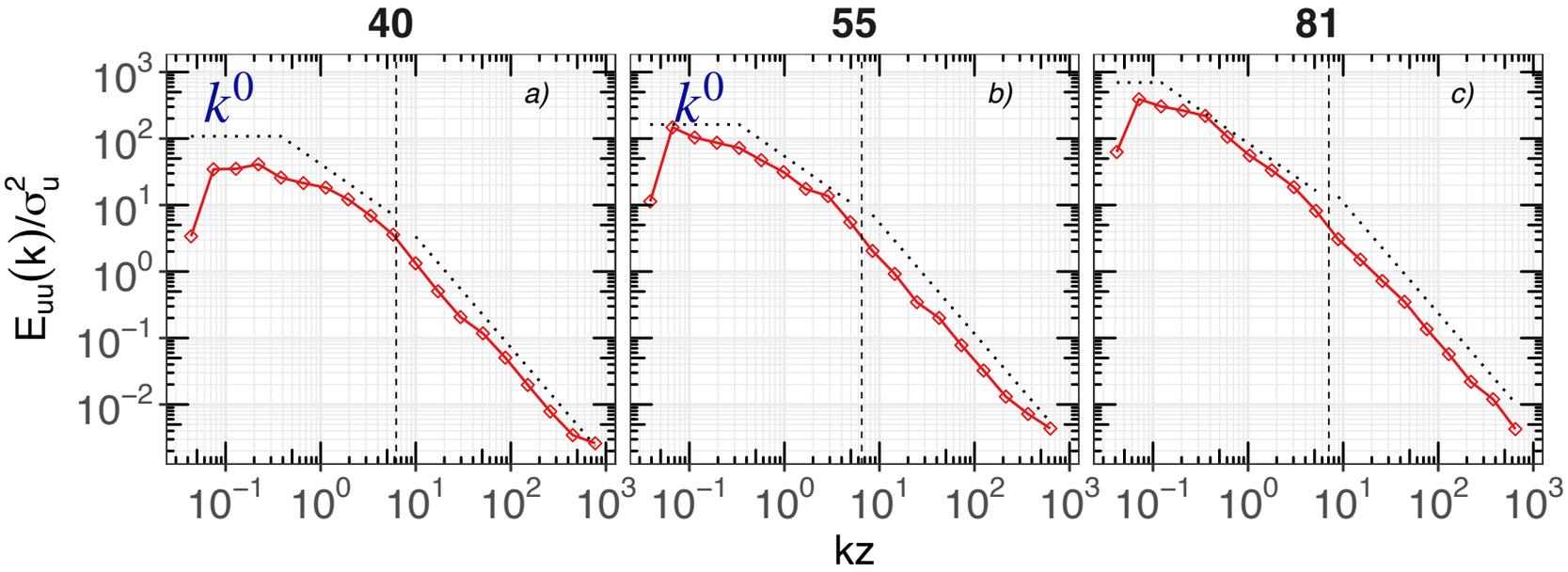

$E_{uu}(k)$ exhibits an extended ISR scaling at all levels for smaller eddies ($kz > 1$). As z/h increases and the influence of RSL turbulence weakens, the onset of a k^{-1} scaling becomes evident at low wavenumbers ($kz < 1$) suggestive of dominance of attached eddies.

$E_{ww}(k)$ also exhibits an extended ISR scaling for $kz > 1$ at all z. At $kz < 1$, the emerging picture is rather different. Near the canopy top, the measured $E_{ww}(k)$ is well approximated by the idealized shape. With increasing z/h, deviations from a flat energy-splashing region at $kz < 1$ become noticeable.

Results: Spectral and Cospectral Properties

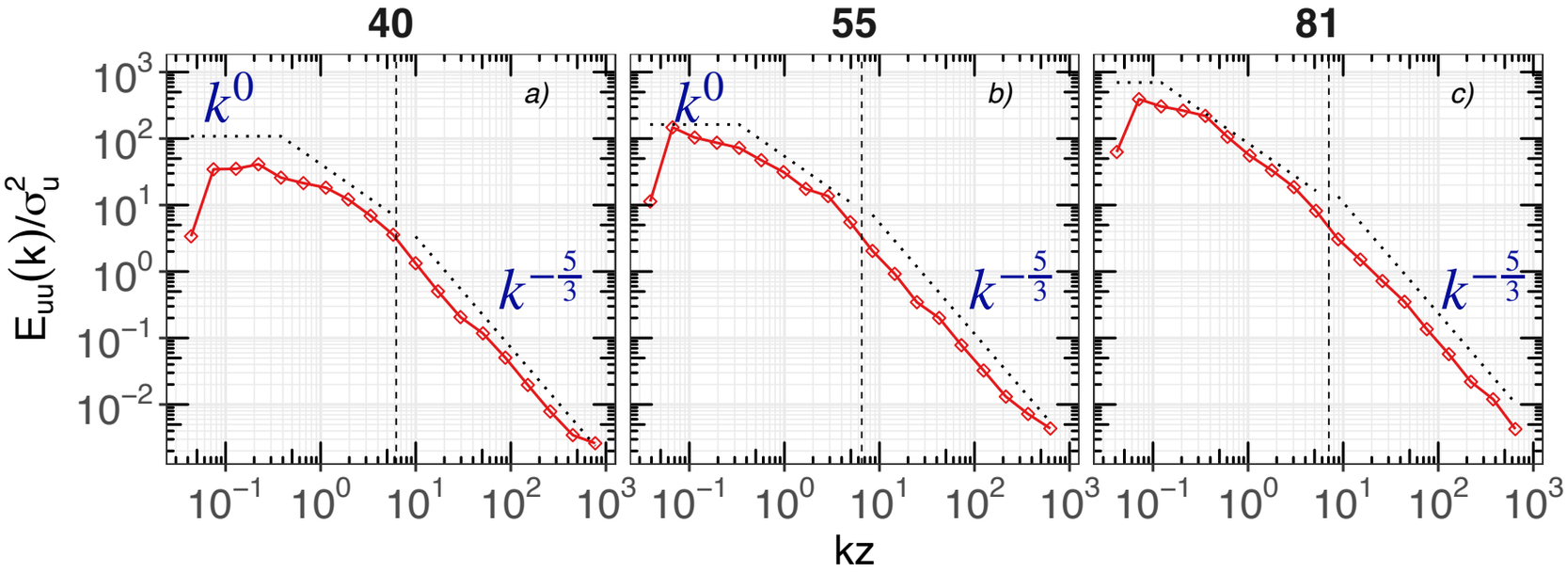

$E_{uu}(k)$ exhibits an extended ISR scaling at all levels for smaller eddies ($kz > 1$). As z/h increases and the influence of RSL turbulence weakens, the onset of a k^{-1} scaling becomes evident at low wavenumbers ($kz < 1$) suggestive of dominance of attached eddies.

$E_{ww}(k)$ also exhibits an extended ISR scaling for $kz > 1$ at all z. At $kz < 1$, the emerging picture is rather different. Near the canopy top, the measured $E_{ww}(k)$ is well approximated by the idealized shape. With increasing z/h, deviations from a flat energy-splashing region at $kz < 1$ become noticeable.

Results: Spectral and Cospectral Properties

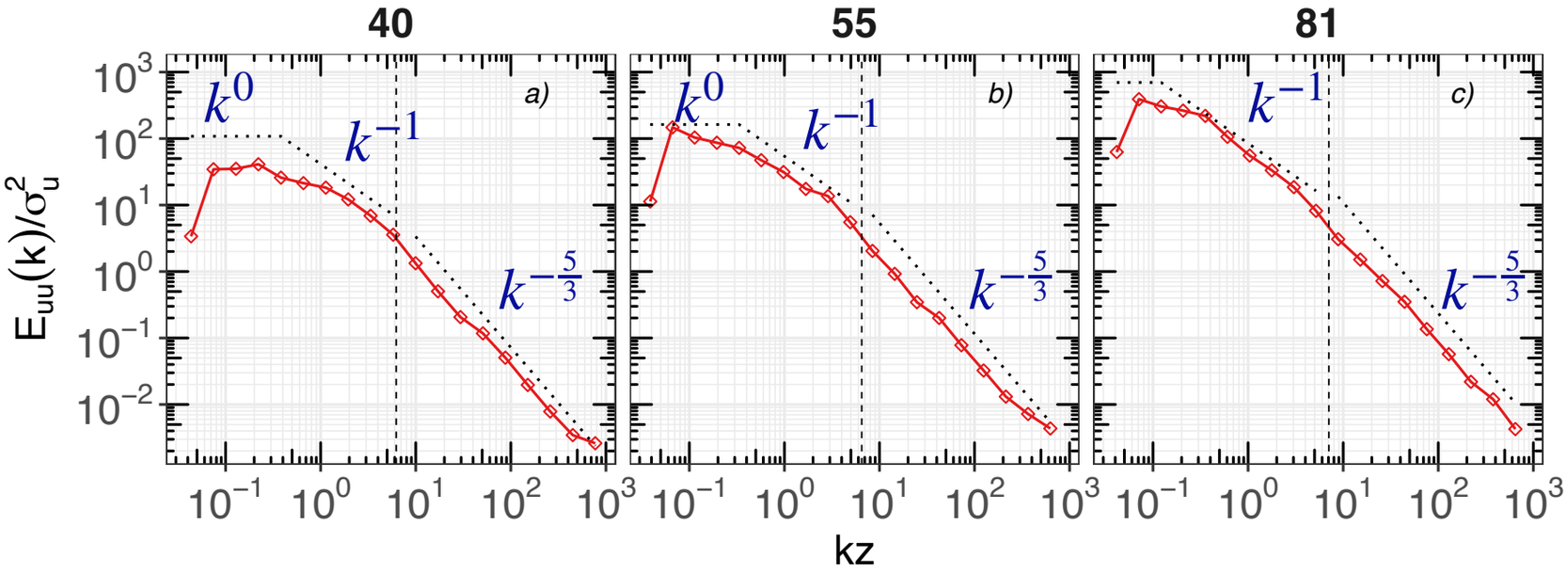

$E_{uu}(k)$ exhibits an extended ISR scaling at all levels for smaller eddies ($kz > 1$). As z/h increases and the influence of RSL turbulence weakens, the onset of a k^{-1} scaling becomes evident at low wavenumbers ($kz < 1$) suggestive of dominance of attached eddies.

$E_{ww}(k)$ also exhibits an extended ISR scaling for $kz > 1$ at all z. At $kz < 1$, the emerging picture is rather different. Near the canopy top, the measured $E_{ww}(k)$ is well approximated by the idealized shape. With increasing z/h, deviations from a flat energy-splashing region at $kz < 1$ become noticeable.

Results: the relaxation time scale

$$\tau(k) = \alpha\epsilon^{-1/3}k^{-2/3}$$

$$F_{wu}(k) = -A^{-1}\frac{dU}{dz}\tau(k)E_{ww}(k)$$

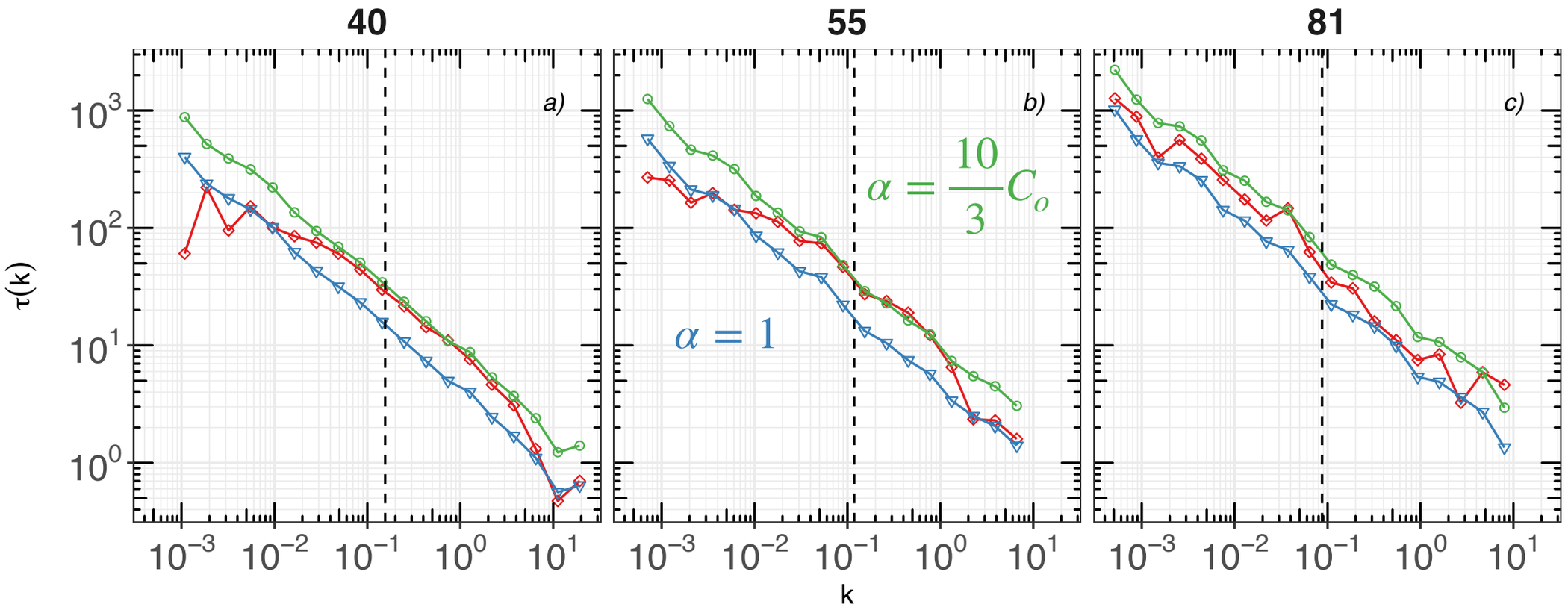

For $kz \ll 1$ and $z/h < 2$, the agreement indicates that $\tau(k)$ is independent of k (i.e. measured $\tau(k)$ scales as k^0 instead of $k^{-2/3}$). This independence at $kz \ll 1$ from k may be hinting that canopy scale processes are restricting τ at large scales for $z/h = 1$. Clearly, these restrictions become weaker with increasing z/h.

Results: CSB model assessment

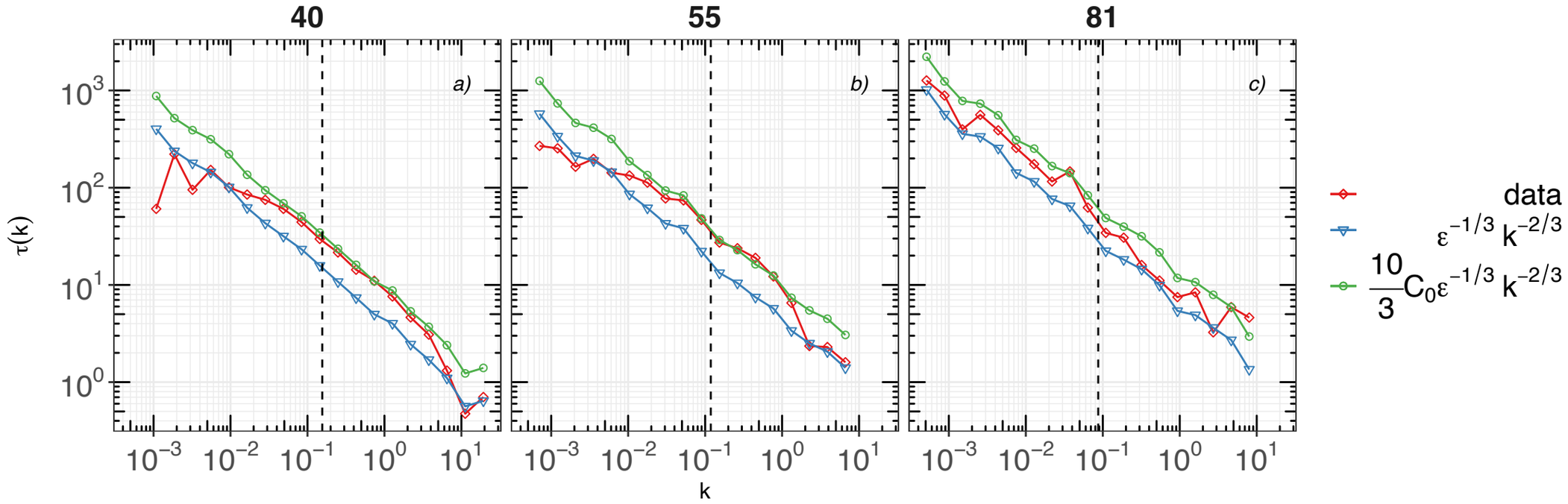

Results: CSB model assessment

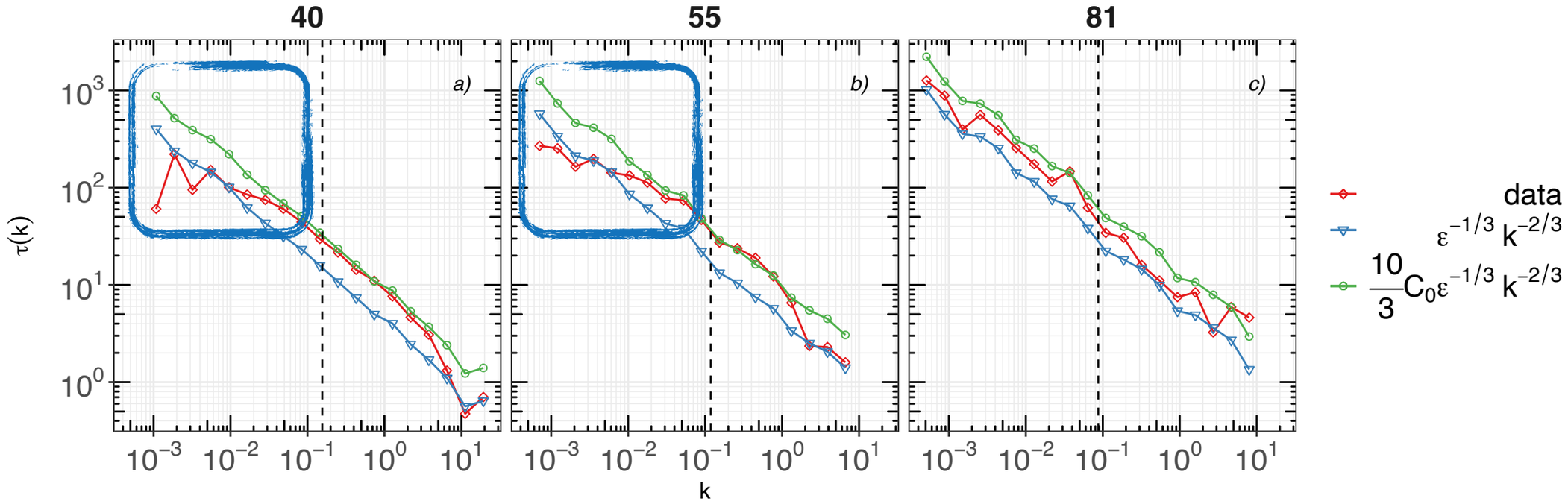

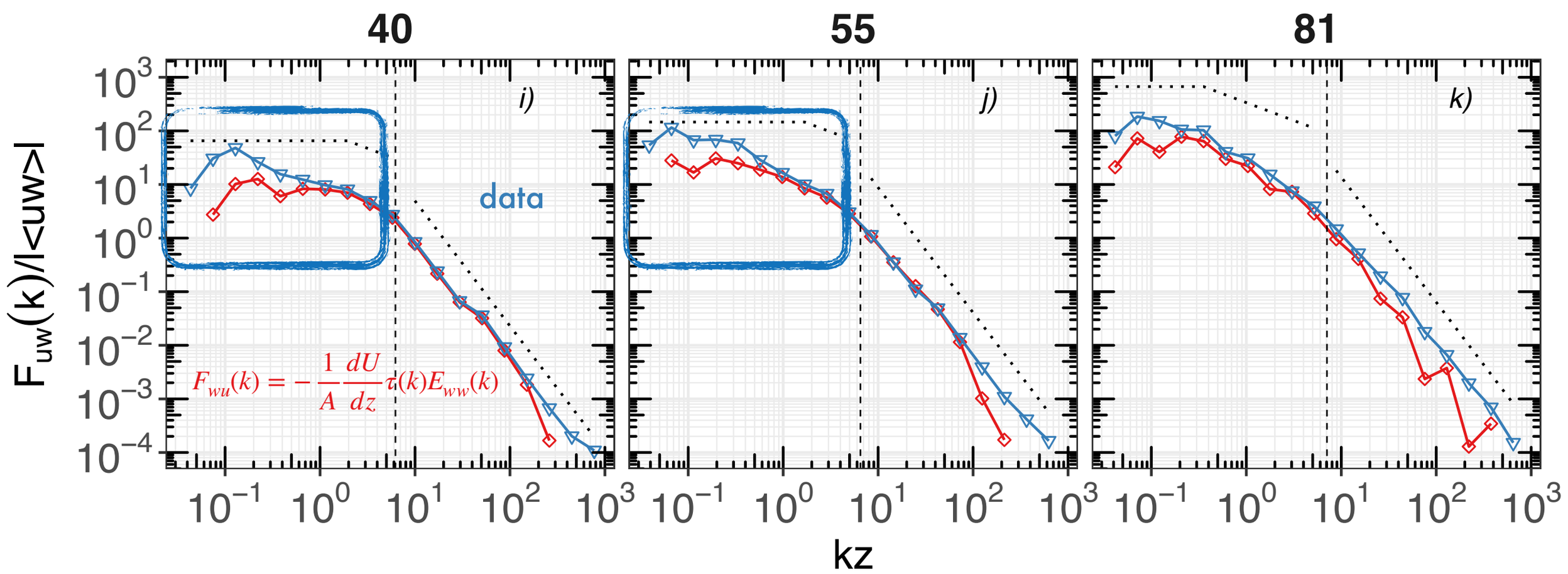

Results: Spectral and Cospectral Properties

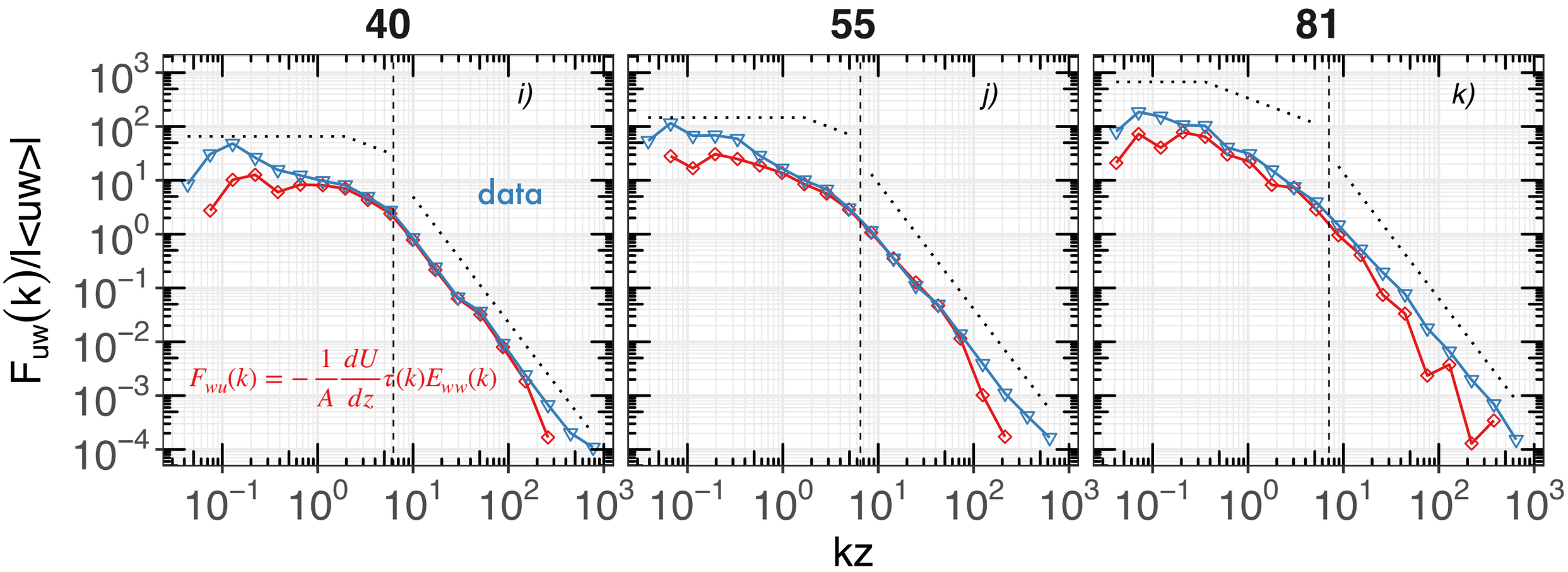

The notable difference between measured and modeled $F_{uw}(k)$ is at $kz \ll 1$. Because $\tau(k) = \alpha\epsilon^{-1/3}k^{-2/3}$, a $k^{-2/3}$ scaling is expected in modeled $F_{uw}(k)$ when $E_{ww}(k)$ experiences a k^0 regime. However, the measured $F_{uw}(k)$ does not support a $k^{-2/3}$ scaling near the canopy top at $kz < 1$. Nonetheless, with increasing z/h, the measured and predicted $F_{uw}(k)$ do agree better at the low wavenumber end. Not withstanding this issue at low k, the overall agreement between measured and modeled $F_{uw}(k)$ are acceptable for linking ϕ_{RSL} to $E_{ww}(k)$.

Results: Spectral Peaks and the dissipation length scale, L_d

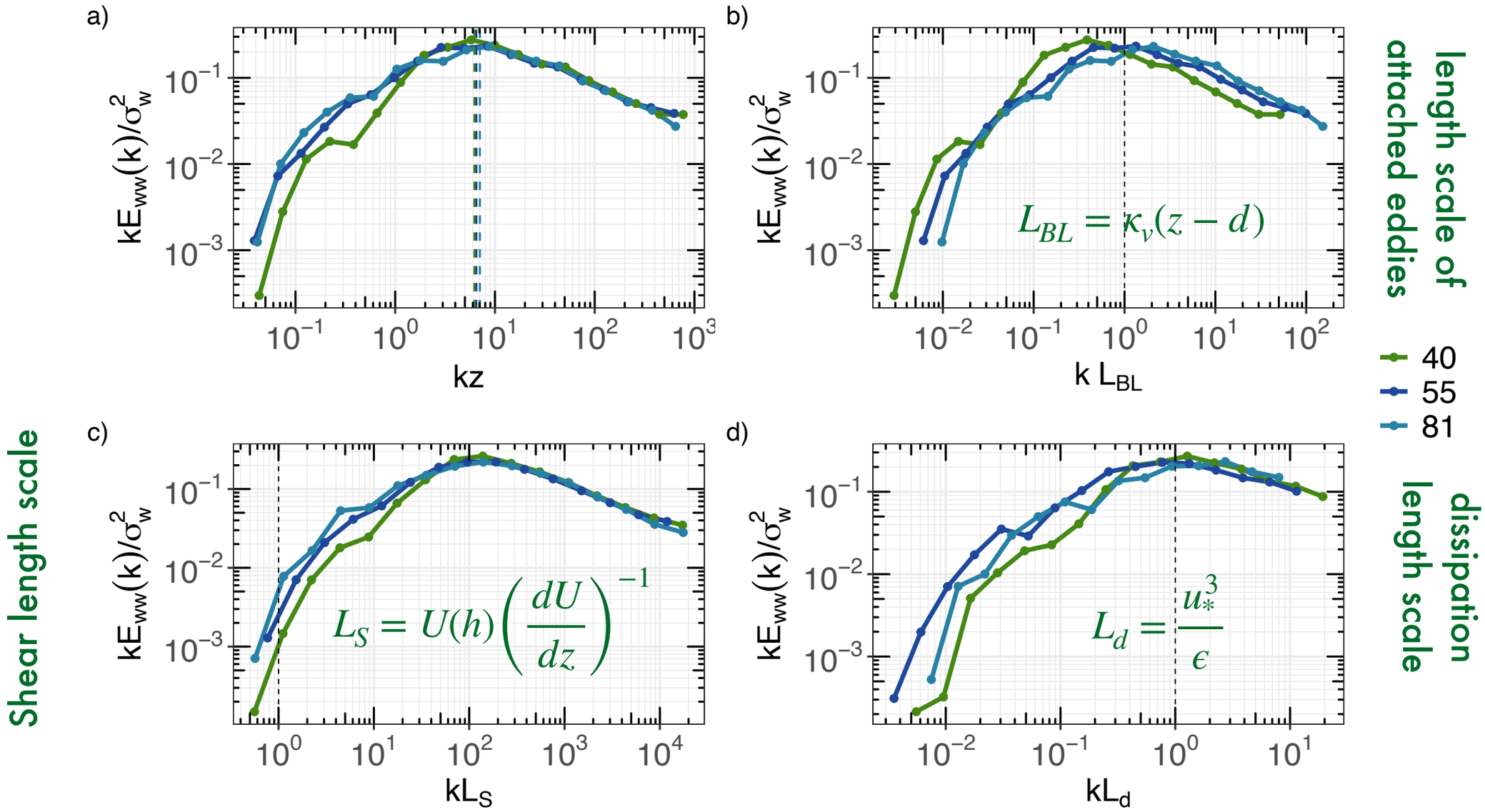

At all z, a k_a that can be reasonably identified from the maximum of $kE_{ww}(k)/\sigma_w^2$.
This analysis provides experimental support to the finding $k_a L_d \approx 1$.

Results: Spectral Peaks and the dissipation length scale, L_d

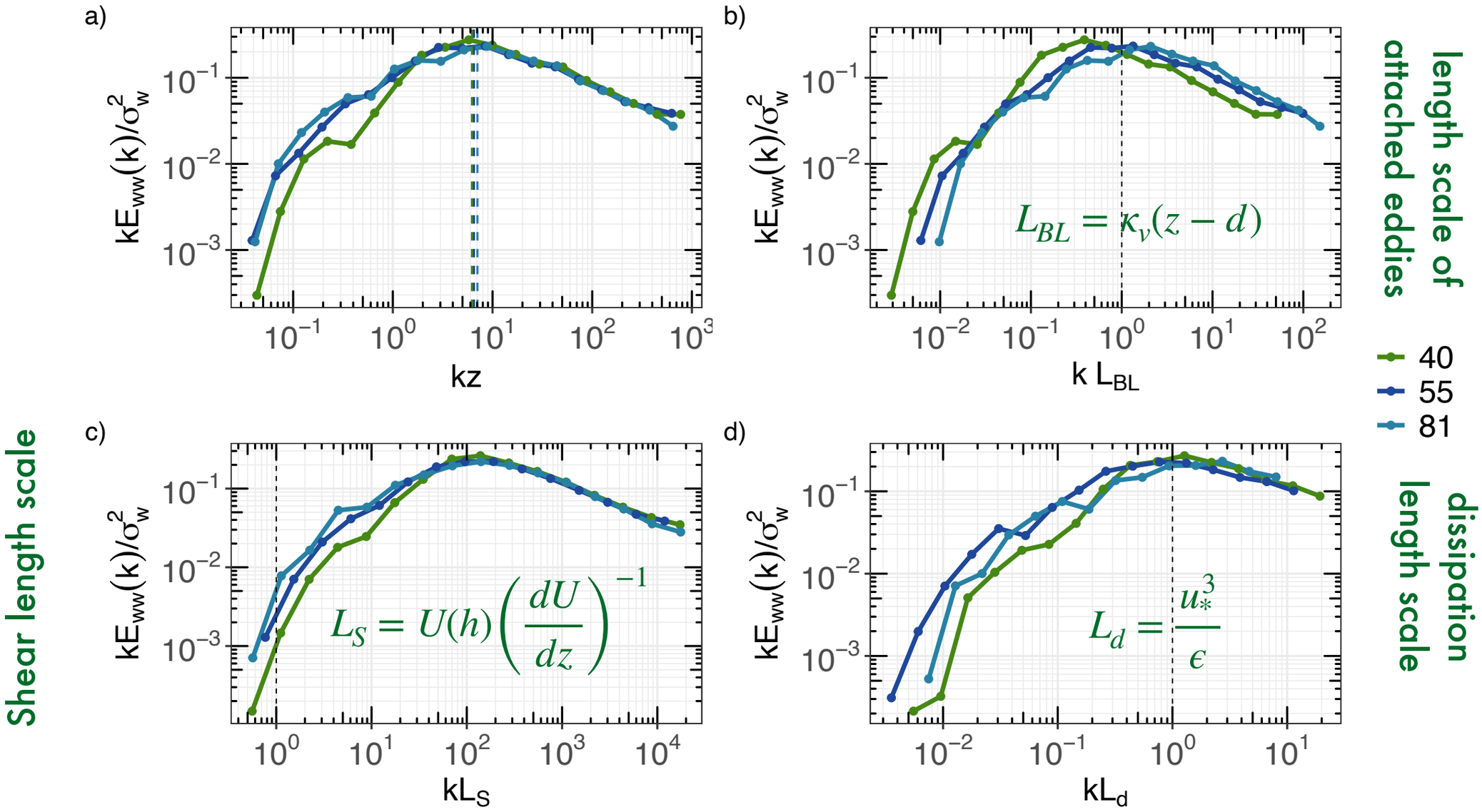

At all z, a k_a that can be reasonably identified from the maximum of $kE_{ww}(k)/\sigma_w^2$.
This analysis provides experimental support to the finding $k_a L_d \approx 1$.

$$\frac{1}{k_a L_d} = \left[\left(\frac{2}{5C_o}\right)^{1/2}\left(\frac{\sigma_w}{u_*}\right)\right]^3 .$$

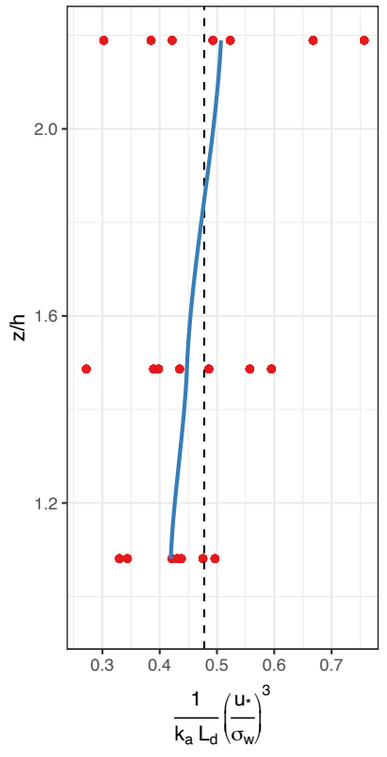

Results: ϕ_{RSL} model predictions

$$\phi_{RSL} = \frac{\kappa_v (z-d) dU}{u_* \quad dz}$$

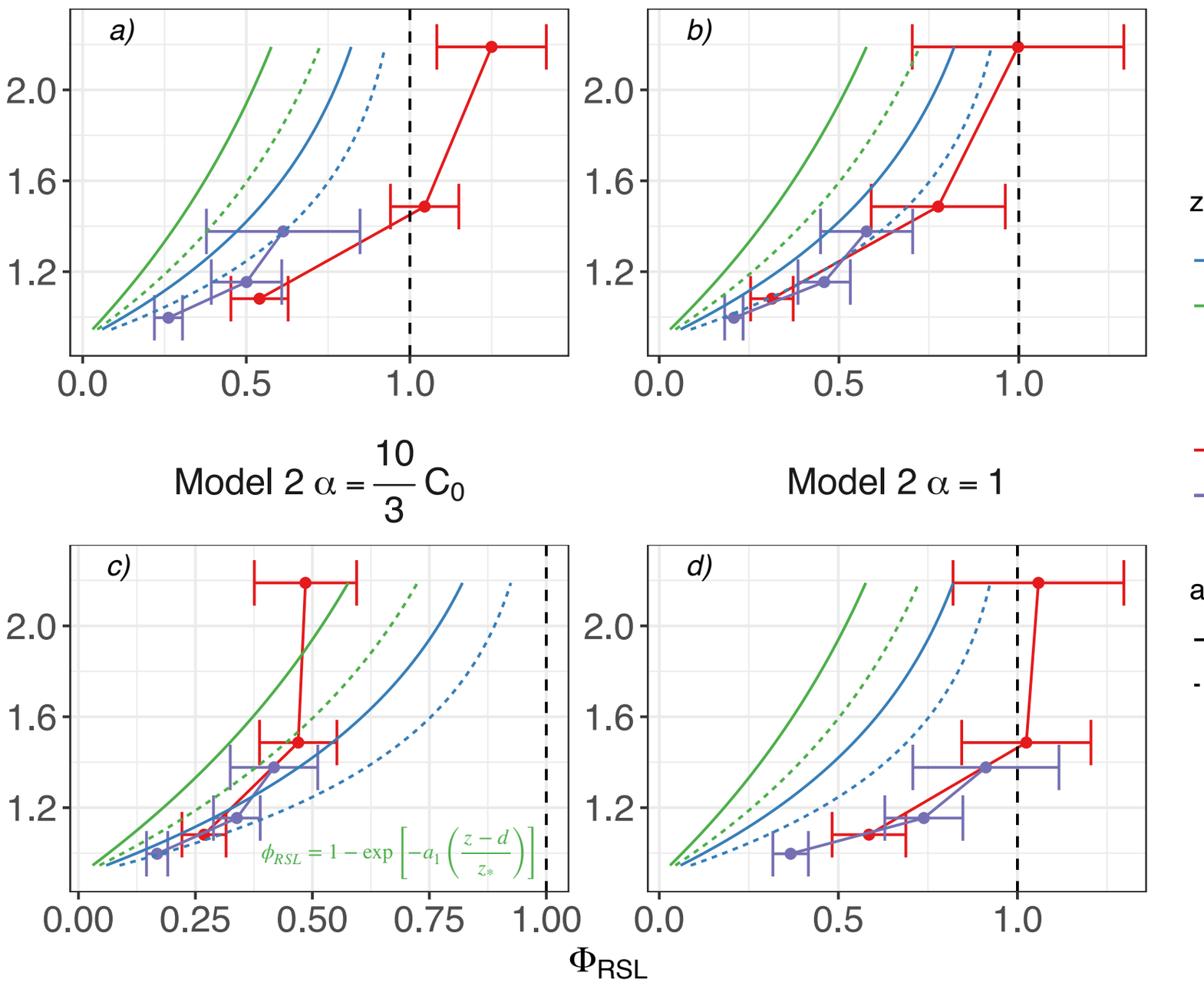

$$\phi_{RSL} = \begin{cases} -\frac{A}{2}\frac{\overline{u'w'}}{u_*^2}\left(\frac{u_*}{\sigma_w}\right)^4 \frac{L_{BL}}{L_d} \\ -\frac{5}{3}\frac{AC_o}{\alpha}\left(\frac{\overline{u'w'}}{u_*^2}\right)\left(\frac{u_*}{\sigma_w}\right)^4 \frac{L_{BL}}{L_d} \end{cases}$$

$$\phi_{RSL} = -A\left(\frac{\overline{u'w'}}{u_*^2}\right)\left(\frac{u_*\, L_{BL}}{\int_0^\infty \tau(k) E_{ww}(k) dk}\right)$$

Discussion and Conclusions

Three models for ϕ_{RSL} are proposed:

Discussion and Conclusions

Three models for ϕ_{RSL} are proposed:

- The first uses a simplified turbulent momentum flux budget along with standard closure schemes.

Discussion and Conclusions

Three models for ϕ_{RSL} are proposed:

- The first uses a simplified turbulent momentum flux budget along with standard closure schemes.
- The second uses a 'spectral' version of the same approach and establishes a link between ϕ_{RSL} and the spectrum of the vertical wind velocity.

Discussion and Conclusions

Three models for ϕ_{RSL} are proposed:

- The first uses a simplified turbulent momentum flux budget along with standard closure schemes.
- The second uses a 'spectral' version of the same approach and establishes a link between ϕ_{RSL} and the spectrum of the vertical wind velocity.
- The third adopts idealized shapes for the spectrum of vertical velocity in the RSL thereby enabling an analytical link between ϕ_{RSL} and the dissipation length scale, L_d.

Discussion and Conclusions

Discussion and Conclusions

The mixing layer analogy is not used (possible extension to sparse canopies and urban canopy).

Discussion and Conclusions

The mixing layer analogy is not used (possible extension to sparse canopies and urban canopy).

Because the turbulent kinetic energy dissipation rate is conserved across $E_{ww}(k)$, the CSB model reveals a novel link between ϕ_{RSL} and L_{BL}/L_d.

Discussion and Conclusions

The mixing layer analogy is not used (possible extension to sparse canopies and urban canopy).

Because the turbulent kinetic energy dissipation rate is conserved across $E_{ww}(k)$, the CSB model reveals a novel link between ϕ_{RSL} and L_{BL}/L_d.

The CSB model unambiguously shows that the appropriate eddy viscosity that applies simultaneously in the RSL and ISL is given by: $\nu_t = \dfrac{1 - C_I}{C_R} \displaystyle\int_0^\infty \tau(k) E_{ww}(k) dk,$

Discussion and Conclusions

The mixing layer analogy is not used (possible extension to sparse canopies and urban canopy).

Because the turbulent kinetic energy dissipation rate is conserved across $E_{ww}(k)$, the CSB model reveals a novel link between ϕ_{RSL} and L_{BL}/L_d.

The CSB model unambiguously shows that the appropriate eddy viscosity that applies simultaneously in the RSL and ISL is given by: $\nu_t = \dfrac{1 - C_I}{C_R} \int_0^\infty \tau(k) E_{ww}(k) dk,$

It is the conservative nature (i.e. constant ϵ across k) of the energy cascade and the lack of equilibrium between scale-wise energy production and energy dissipation at each k that resulted in L_d being a new length scale needed to describe ν_t and thus ϕ_{RSL}.

Discussion and Conclusions

The mixing layer analogy is not used (possible extension to sparse canopies and urban canopy).

Because the turbulent kinetic energy dissipation rate is conserved across $E_{ww}(k)$, the CSB model reveals a novel link between ϕ_{RSL} and L_{BL}/L_d.

The CSB model unambiguously shows that the appropriate eddy viscosity that applies simultaneously in the RSL and ISL is given by: $\nu_t = \dfrac{1 - C_I}{C_R} \displaystyle\int_0^\infty \tau(k) E_{ww}(k) dk,$

It is the conservative nature (i.e. constant ϵ across k) of the energy cascade and the lack of equilibrium between scale-wise energy production and energy dissipation at each k that resulted in L_d being a new length scale needed to describe ν_t and thus ϕ_{RSL}.

The ϕ_{RSL} behaviour is shown to be partly connected to the fact that moving away from the canopy $E_{ww}(k)$ begins to exhibit a scaling law with an exponent that becomes more negative with increasing z/h but remains larger than k^{-1}.

Thank you!

Cléo Quaresma

Nelson Dias

Gabriel Katul

Marcelo Chamecki

Daniela Cava

l.mortarini@isac.cnr.it

Discussion and Conclusions

Moving Equilibrium Hypothesis:

Discussion and Conclusions

Moving Equilibrium Hypothesis:

At a given x, the u_* at the canopy top becomes a local variable reflecting the overall local balance between friction (or canopy drag), variations in $\overline{P}$ (due to topography) and geostrophic winds. Thus, the moving equilibrium hypothesis sets u_* at the canopy top to be the logical variable to normalize flow statistics in z locally, which is assumed here. Variations in $\overline{w'u'}$ and σ_w in z now introduce vertical scales in ϕ_{RSL} that must be considered.

Discussion and Conclusions

Moving Equilibrium Hypothesis:

At a given x, the u_* at the canopy top becomes a local variable reflecting the overall local balance between friction (or canopy drag), variations in $\overline{P}$ (due to topography) and geostrophic winds. Thus, the moving equilibrium hypothesis sets u_* at the canopy top to be the logical variable to normalize flow statistics in z locally, which is assumed here. Variations in $\overline{w'u'}$ and σ_w in z now introduce vertical scales in ϕ_{RSL} that must be considered.

ϕ_{RSL} can be derived to accommodate variations in $\overline{w'u'}/u_*^2$ and σ_w/u_* as well as any imbalance between production and dissipation of turbulent kinetic energy (i.e. $P_m/\epsilon \neq 1$) with z.

Discussion and Conclusions

Moving Equilibrium Hypothesis:

At a given x, the u_* at the canopy top becomes a local variable reflecting the overall local balance between friction (or canopy drag), variations in $\overline{P}$ (due to topography) and geostrophic winds. Thus, the moving equilibrium hypothesis sets u_* at the canopy top to be the logical variable to normalize flow statistics in z locally, which is assumed here. Variations in $\overline{w'u'}$ and σ_w in z now introduce vertical scales in ϕ_{RSL} that must be considered.

ϕ_{RSL} can be derived to accommodate variations in $\overline{w'u'}/u_*^2$ and σ_w/u_* as well as any imbalance between production and dissipation of turbulent kinetic energy (i.e. $P_m/\epsilon \neq 1$) with z.

Within the moving equilibrium hypothesis, the derivation for ϕ_{RSL} showed that the macro-scale dissipation length scale $L_d = u_*^3/\epsilon$ emerges naturally from a co-spectral budget model. The derivation presumed that ϵ is the quantity that is 'conserved' across the energy cascade of $E_{ww}(k)$ thereby enabling 'generic' description for its shape. The derivation made explicit how ϕ_{RSL} can be related to deviations in $\kappa_v(z-d)/L_d$ from unity using a co-spectral budget model.

Discussion and Conclusions

Low wavenumber effect on ϕ_{RSL}:

The predicted co-spectrum from models for $\tau(k)$ and measured $E_{ww}(k)$ also agree with the measured co-spectrum. However, a ubiquitous feature in the measured $E_{ww}(k)$ (here and elsewhere in vegetated canopy flow studies) is the emergence of a power-law region with increasing z/h in the vicinity of $kz = 1$

Clearly deviations from the assumed shape (splash + Kolmogorov) must be considered when describing ϕ_{RSL}.

Discussion and Conclusions

Low wavenumber effect on ϕ_{RSL}:

The predicted co-spectrum from models for $\tau(k)$ and measured $E_{ww}(k)$ also agree with the measured co-spectrum. However, a ubiquitous feature in the measured $E_{ww}(k)$ (here and elsewhere in vegetated canopy flow studies) is the emergence of a power-law region with increasing z/h in the vicinity of $kz = 1$

Clearly deviations from the assumed shape (splash + Kolmogorov) must be considered when describing ϕ_{RSL}.

A spectral budget at low wavenumbers for $E_{ww}(k)$ with standard spectral closure schemes shows that

$$E_{ww}(k)\begin{cases}\left[\frac{2}{3}\left(\frac{\alpha_t C_R}{1+\alpha_t C_R + b_K}\right)Y_K(k) + C_1 k^{-1-\alpha_t C_R}\right]\tau(k) & \forall k/k_a \ll 1 \\ = \frac{1}{3}\left(\frac{\alpha_t C_R}{\alpha_t C_R - \frac{2}{3}}\right)2E_K(k) & \forall k/k_a \gg 1\end{cases}$$